

Large Angle Beamstrahlung Monitor (LABM) @ SuperB with Si-CNT detector

M. Ambrosio, C. Aramo , G. Bonvicini, M. Masullo and E. Nappi

The LABM provides a set of direct and passive measurements

It is well known that the major technical challenge of the future Super B factories is to produce and maintain colliding beams of a size never achieved before.

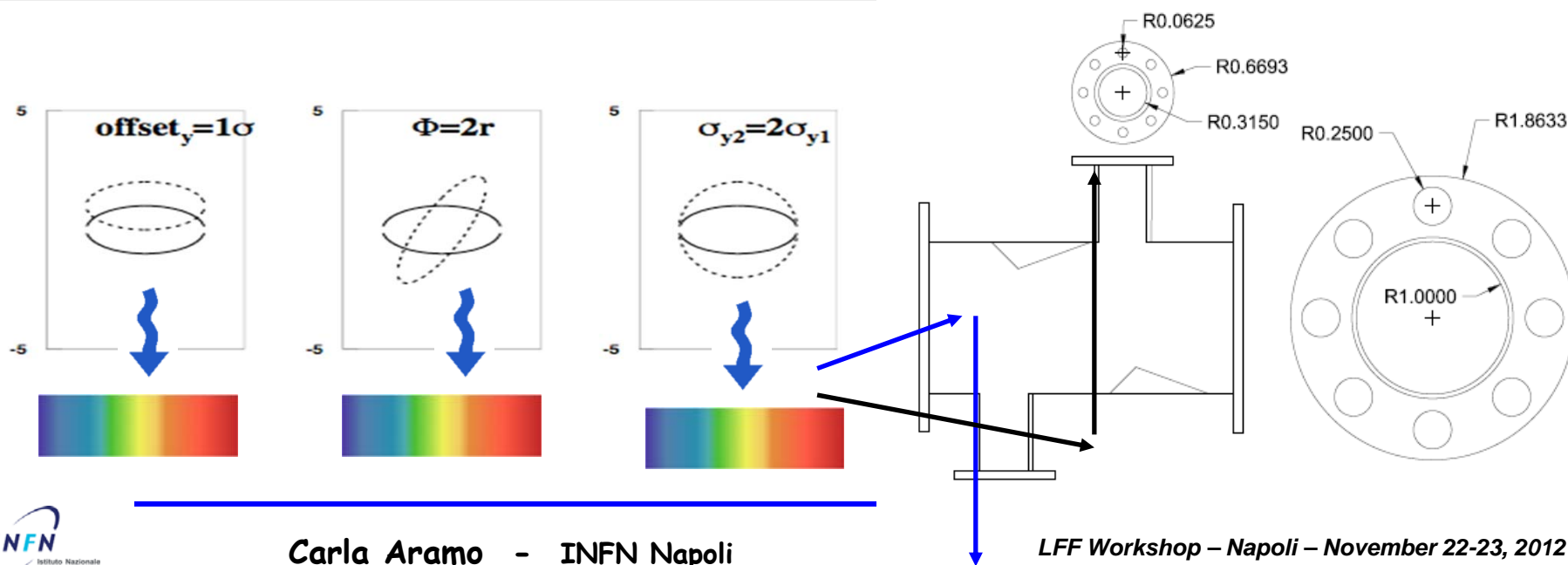
Whereas current e^+e^- storage rings produce beams with transverse heights $y \approx 3 \mu\text{m}$ and widths $x \approx 350 \mu\text{m}$, the new factories nominal parameters are 50 nm and 10 μm respectively.

Even at the relatively large sizes of today's beams, transverse mismatches reduce and ultimately limit the machine's luminosity.

The LABM measures the beamstrahlung light emitted at large angle (large compared to the typical $1/\gamma$ angle of radiation produced by ultra relativistic beams), and relates it to beam parameters so that the beam-beam collision can be optimized for luminosity.

Ground motion: LABM vs luminosity monitor

- A luminosity monitor does not pick out higher corrections. If luminosity decreases due to defocussing, and luminosity feedback is activated, the luminosity will decrease further
- Even if the motion is purely offset-y, a luminosity monitor will not specify whether the correction is up or down
- LABM can produce an asymmetry, $A_{u-d}=(R_u-R_d)/(R_u+R_d)$, which will specify the direction of deflection. For offset-y=1nm, $\theta=7.5\text{mrad}$, and the UV PMTs, $A_{u-d}=0.01-0.02$, recorded on two sides and two polarizations



Large angle beamstrahlung power

At the future B factories, beamstrahlung is abundantly produced (5.4 and 1.3 kW total radiated power for the SuperKEKB HER and LER respectively), and small ($2 \times 2.8 \text{ mm}^2$) 45 degrees mirrors placed inside the Beam Pipe at 7 and 8 mrad and located at ± 90 degrees in azimuth will intercept of the order of 10^{12} beamstrahlung visible photons per second at nominal conditions.

Such abundant signal will provide a lot of opportunity to precisely measure beam parameters.

$$\frac{d^2 I}{d\Omega d\omega} = \frac{3\sigma_z}{4c\pi\sqrt{\pi}} P_0 \frac{1}{\gamma^4 \theta^4} \exp\left(\frac{-\omega^2 \theta^4 \sigma_z^2}{16c^2}\right)$$

Optics Box – Grating mirrors

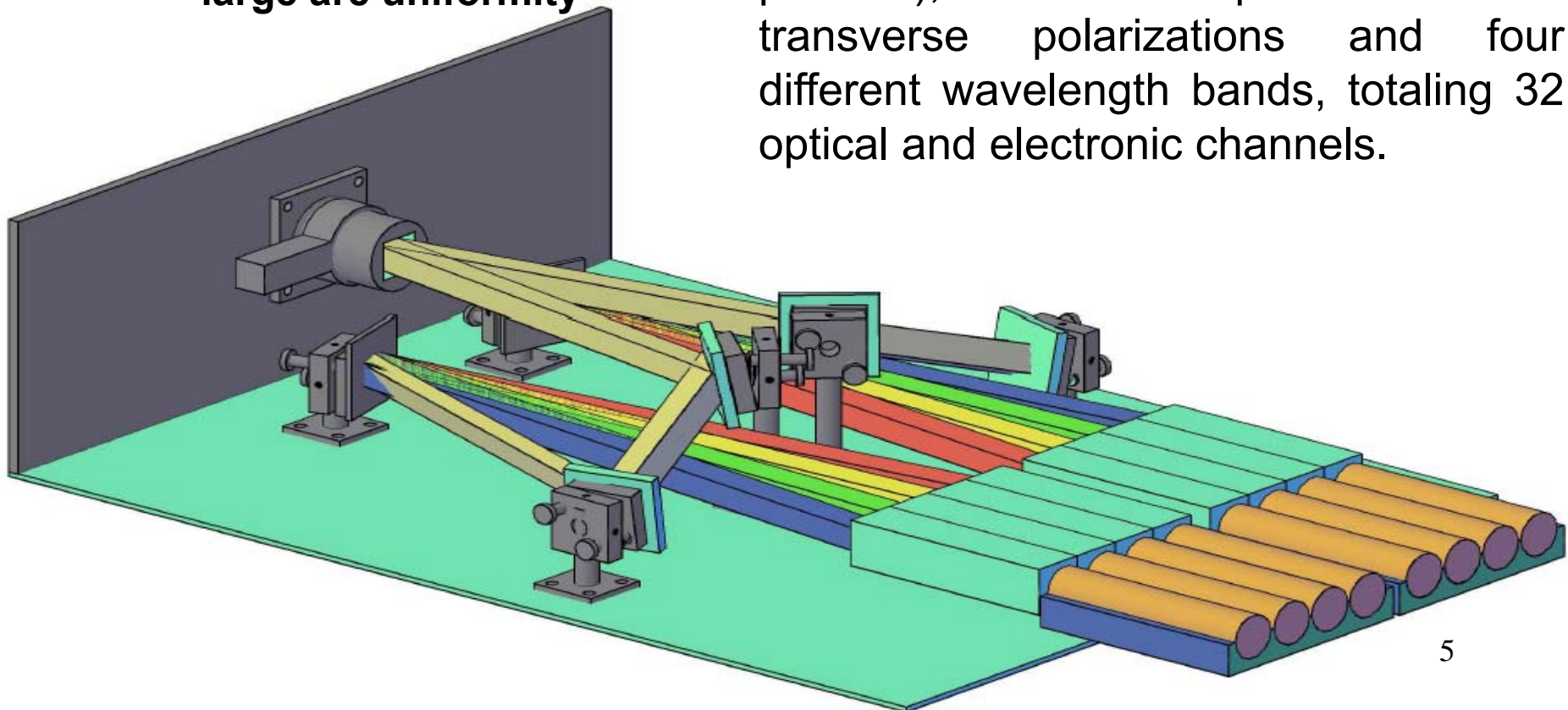
Mirrors = 1 cm²

UV Intensity = 10¹² photons/sec

**Detector: High UV photoresponsivity
large area uniformity**

The monitor consists of four viewports, located at the top and bottom of the beam pipe.

Each viewport is a 2 X 2.8 mm² primary mirror, reflecting light out of the beam pipe. Light is transported through an optical channel to an optical box (one box serves each side, or two viewports per box), where it is separated into two transverse polarizations and four different wavelength bands, totaling 32 optical and electronic channels.

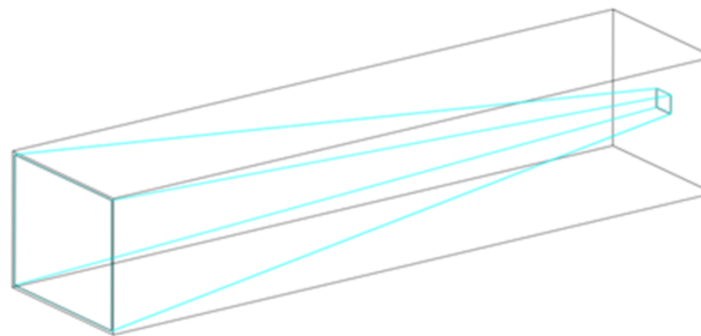
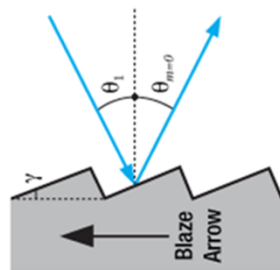
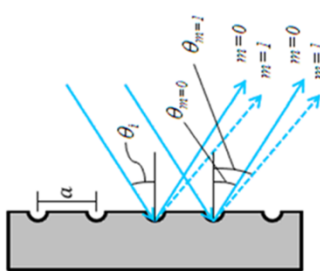


Light Collector and grating

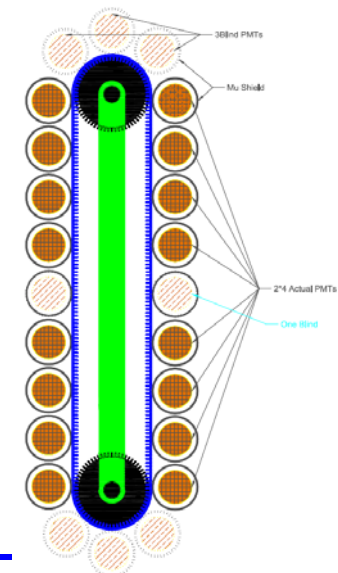
The light is split into two polarizations by a wide band Wollaston prism, and each polarization is spread onto four counters by a ruled grating, which maximizes the reflected intensity in the first order peak. By changing just the grating and the photodetectors, this device can monitor the intervals $225 < \lambda < 495$ nm (UV), $300 < \lambda < 660$ nm (VIS), and $400 < \lambda < 880$ nm (IR). The individual light beams are concentrated by light collectors so that both large photon counters (PMTs) and Si-PMTs can be used.

Normal Reflecting Grating

Ruled or Blazed Grating

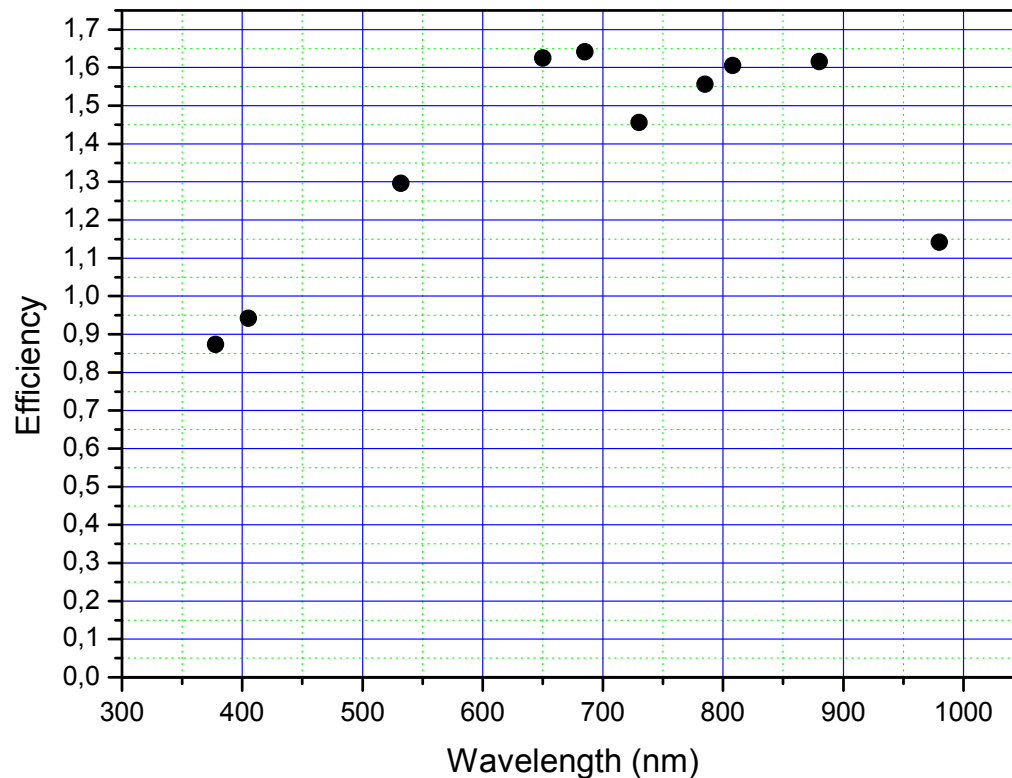


The reason we use such a grating is because ruled gratings have higher efficiencies (or intensities) in the first peak.



Photodetector to be used

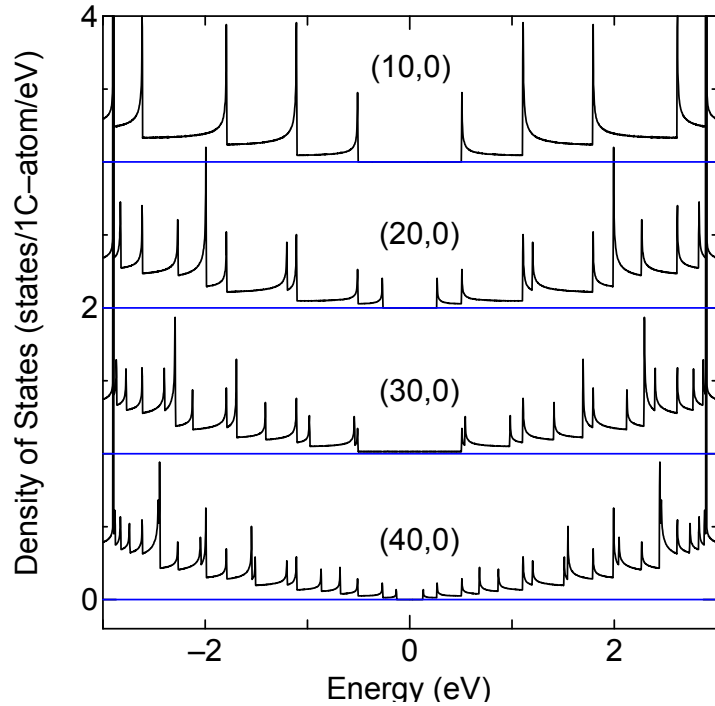
For an efficient reconstruction of beam light intensity and frequency, the ideal detector has to be one with high efficiency in all the wavelength range 225 – 880 nm. It is not necessary to detect single photon, due to the high beam intensity. The ideal would be a photodetector with a quite uniform efficiency in all the range.



Very preliminary result of the last production of Si-CNT photodetector

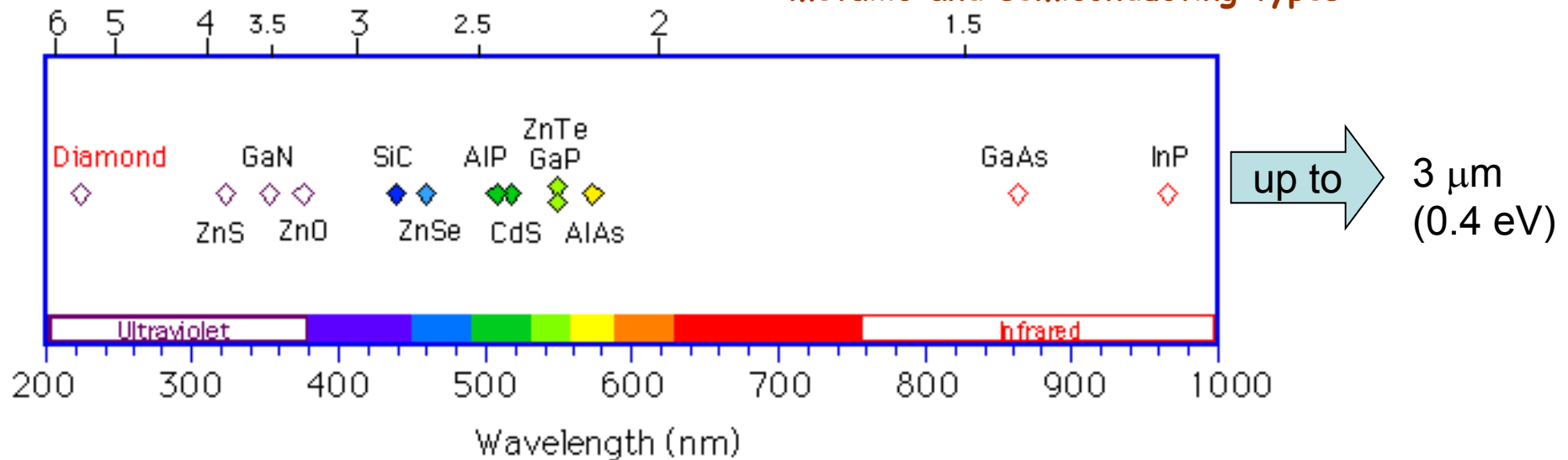
In the following it will be described the main characteristics of Si-CNT photodetectors developed by the INFN collaboration SinPhoNIA.

May CNT be used as photodetectors?

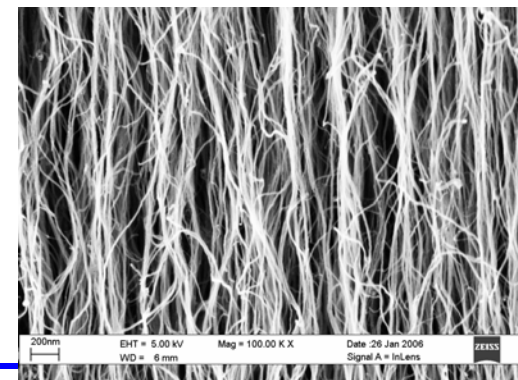
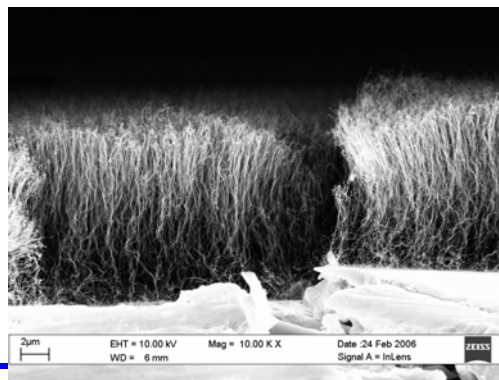
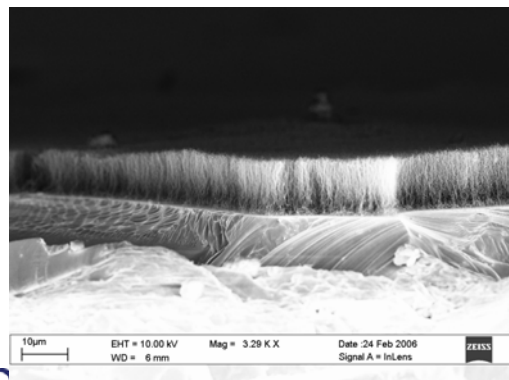
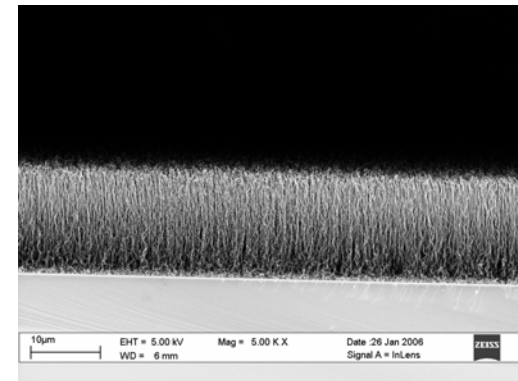
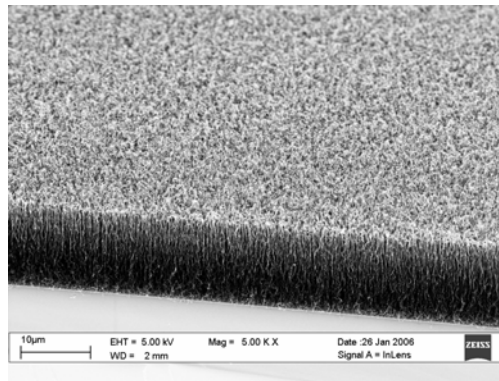
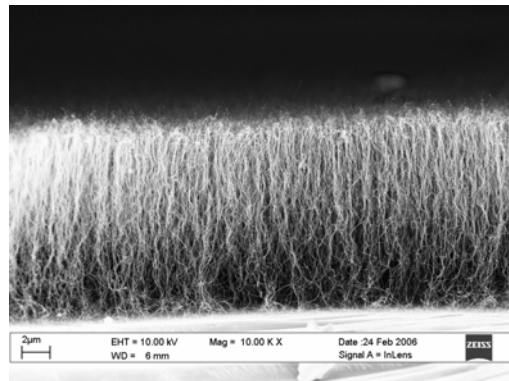
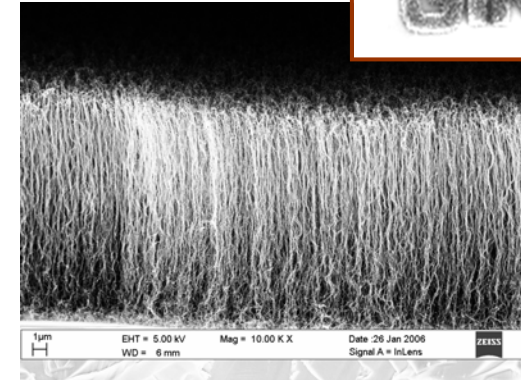
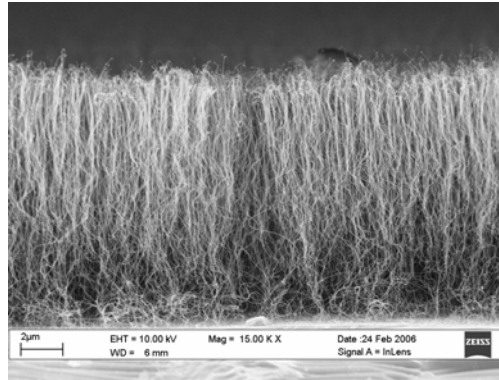
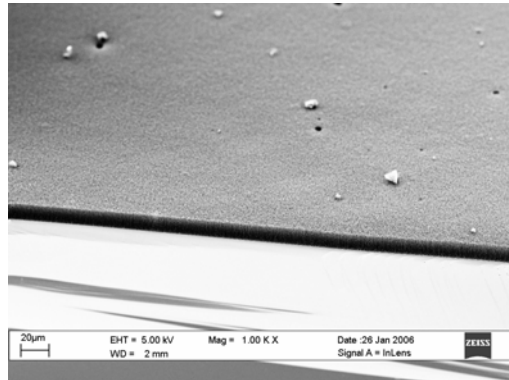


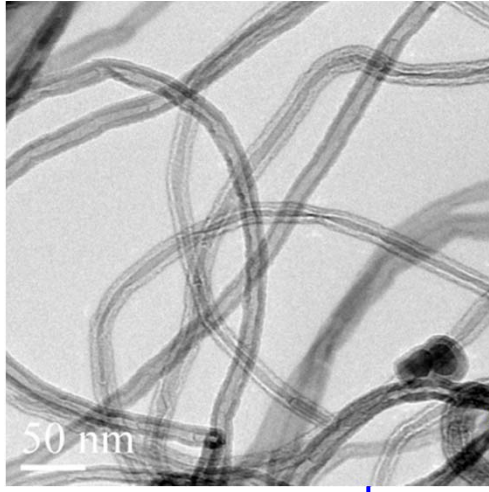
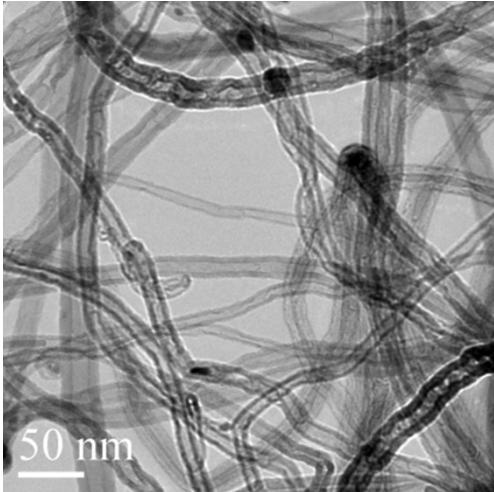
A layer of Multiwall Carbon Nanotubes covers a wide range of diameters and chirality, offering a device sensitive to a wide range of radiation frequencies. In addition the CNT density is very high, allowing, even in a small area, a great number of tubes sensitive to the radiation: $\approx 10^8 - 10^{10}$ MWCNT / 1 mm^2

A multiwall carbon nanotube typically consists of a concentric set of nanotubes of both metallic and semiconducting types



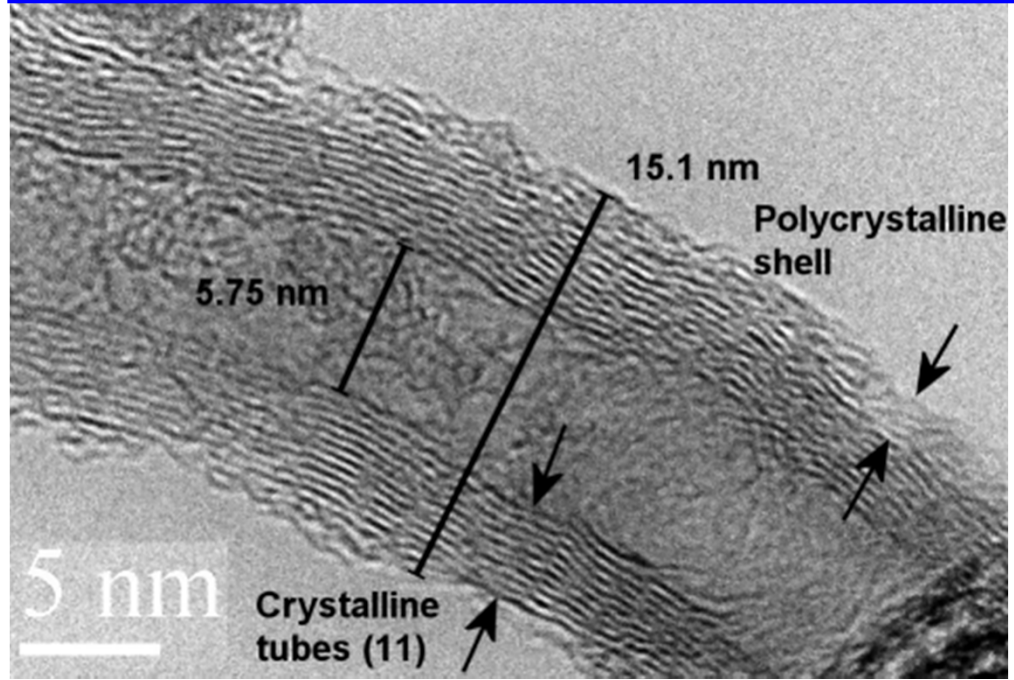
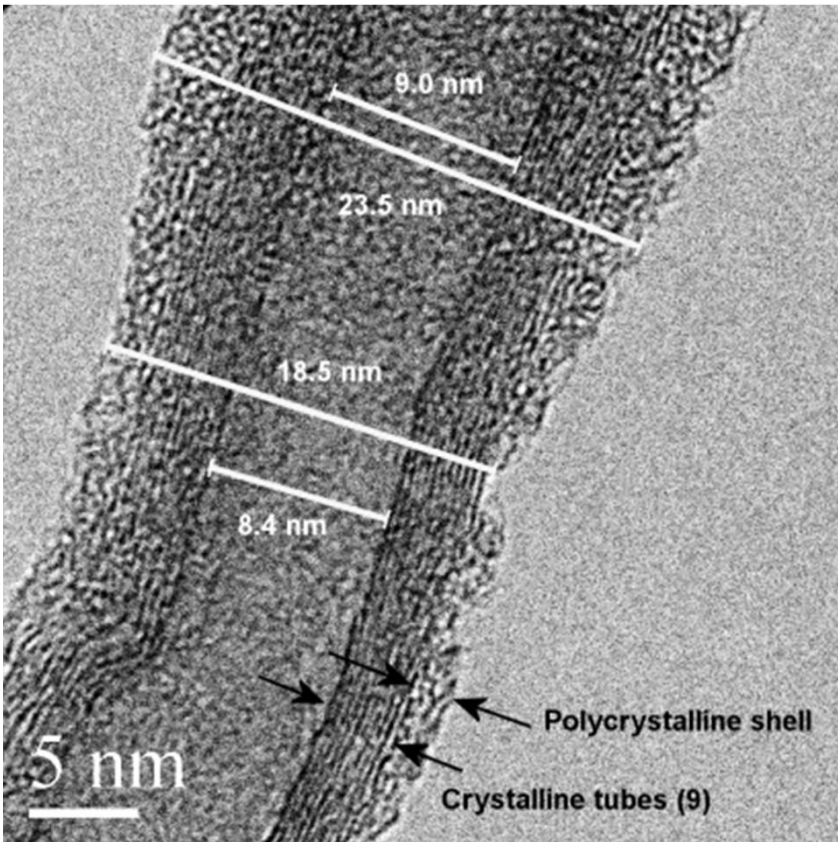
SEM Images



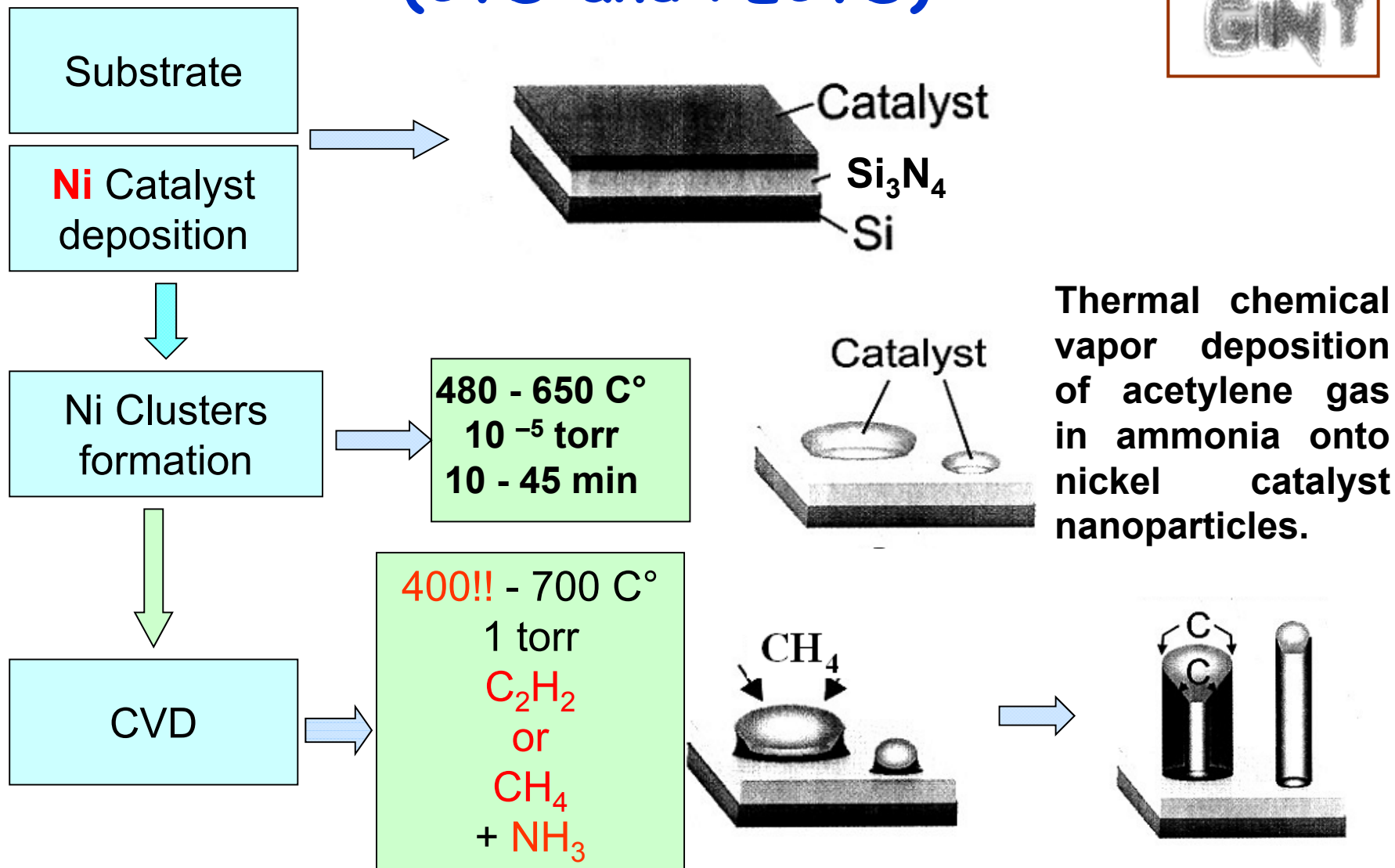


- External diameter: 15 – 25 nm
- Internal diameter: 5 – 10 nm
- Average number of nanotubes: 10 – 15

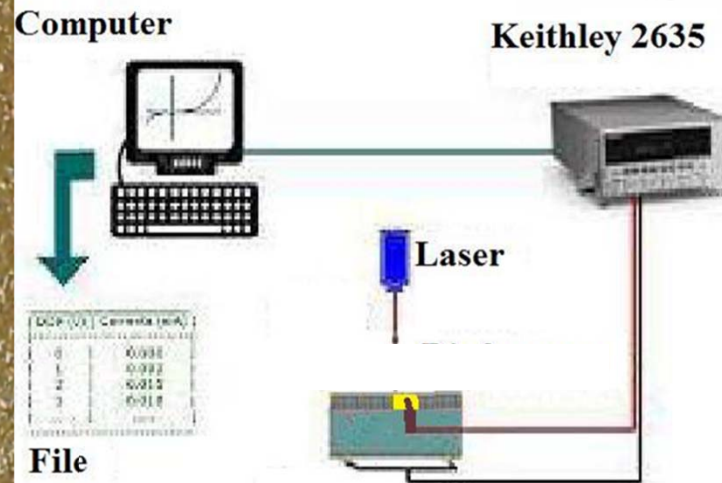
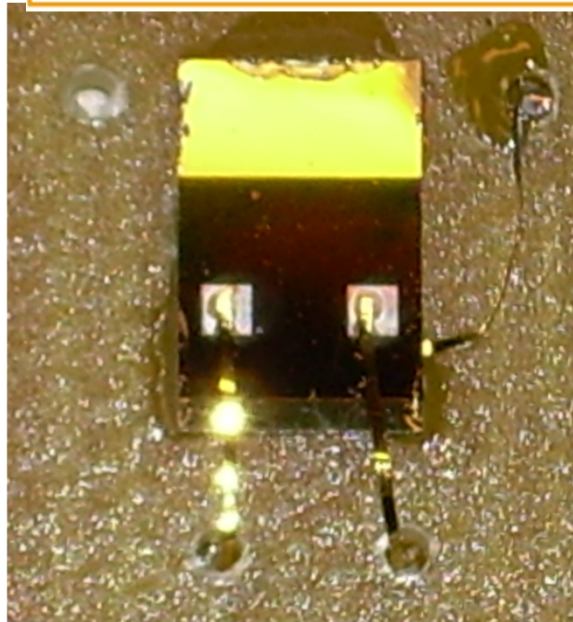
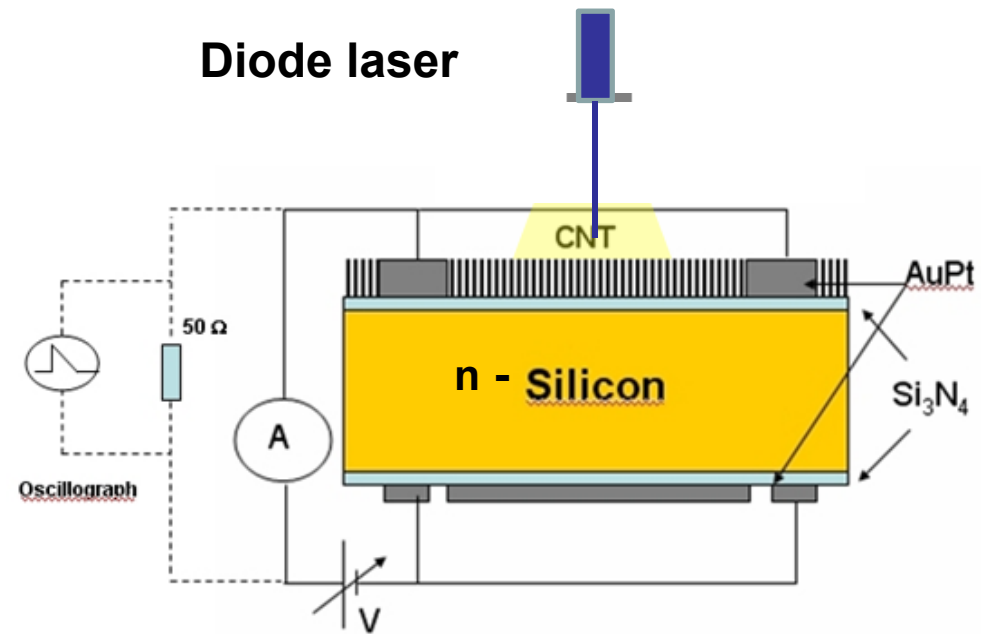
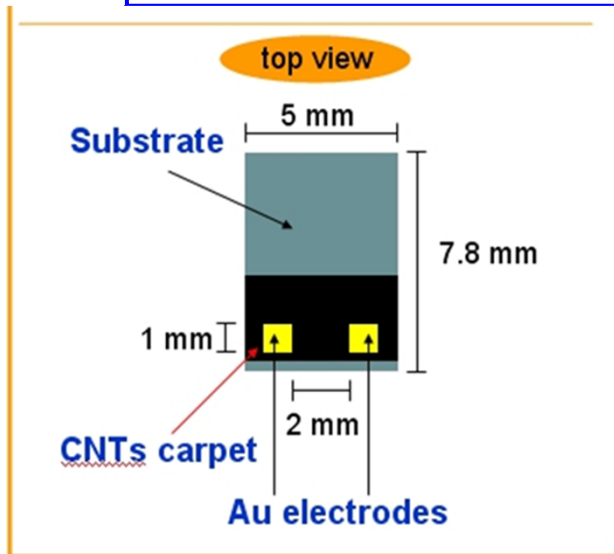
CNT Characteristics



Growth Mechanism of Carbon Nanotubes (CVD and PECVD)



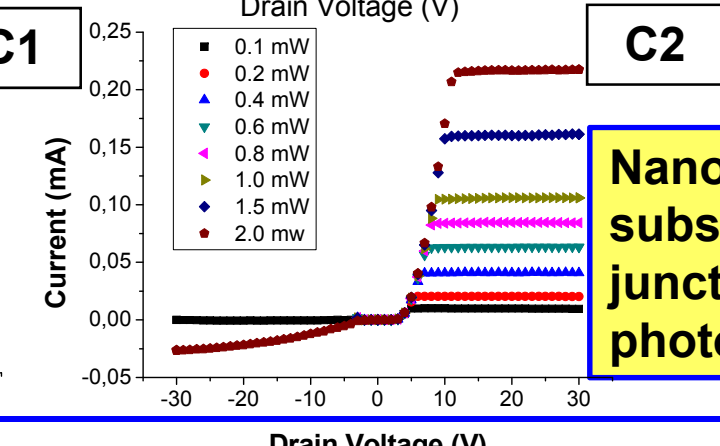
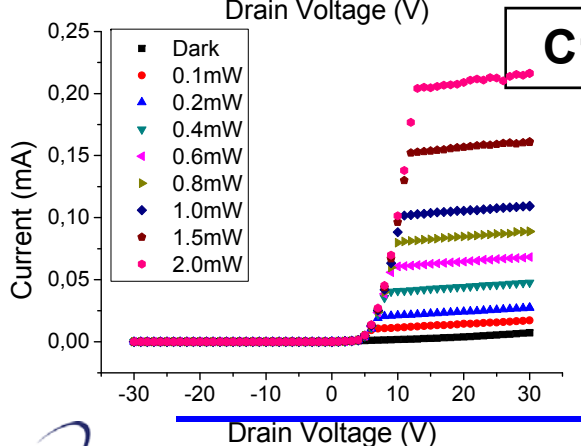
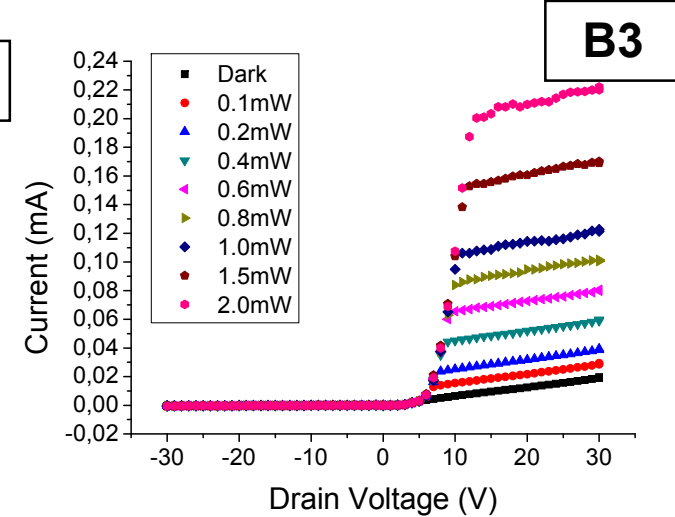
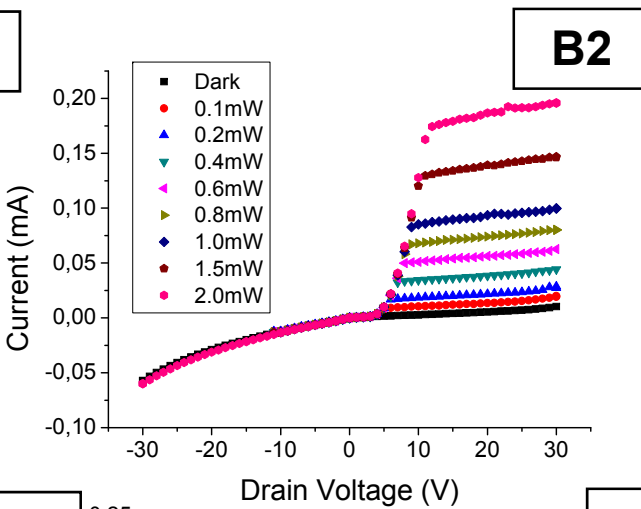
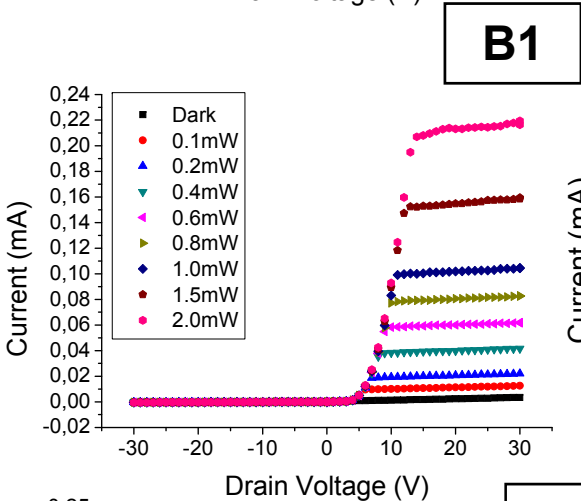
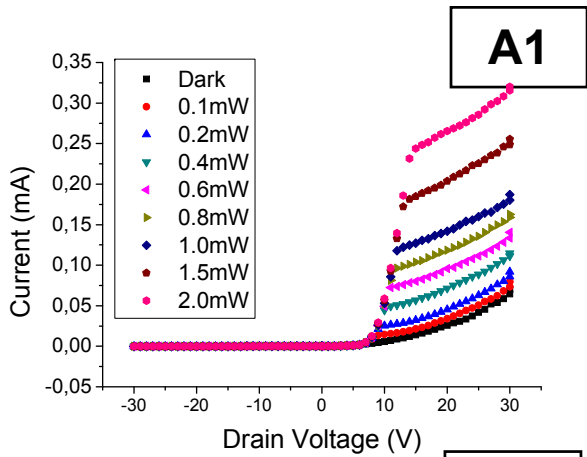
Silicon-CNT radiation detector



In order to investigate the device behavior as radiation detector we equipped a measurement system with LED lasers with a diameter spot of 500 μ m on the sample surface and emitting at various wavelength.

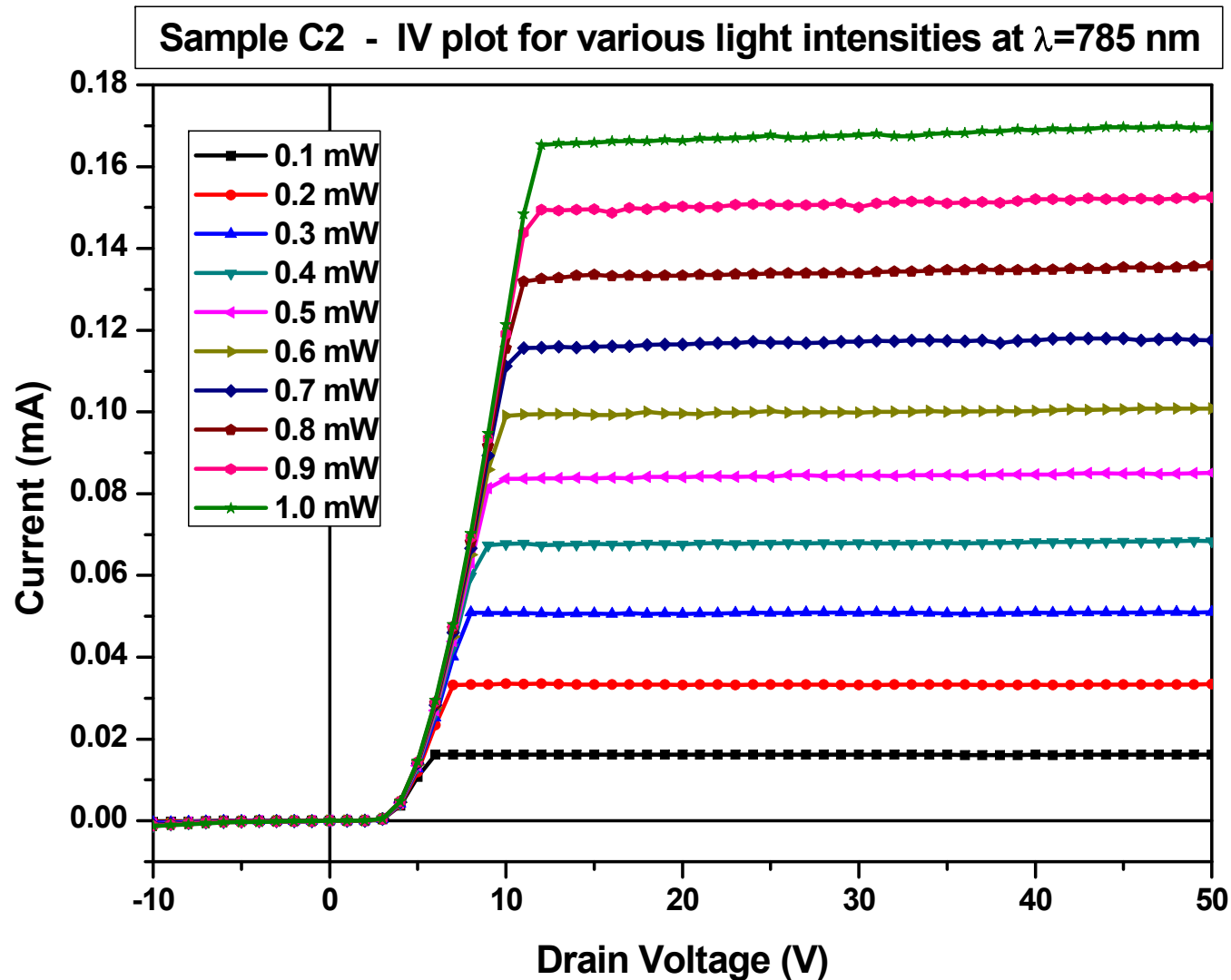
$T_{CVD} = 500 \text{ }^\circ\text{C}$

Room temperature



Nanotubes grown on a silicon substrate create an hetero-junction with surprising photoresponsivity properties.

I-V plot of C2 detector @ $\lambda=785$ nm



Room temperature

No electronics

No signal amplification

Long and stable plateau

Linearity I vs P

Threshold 3.55 V

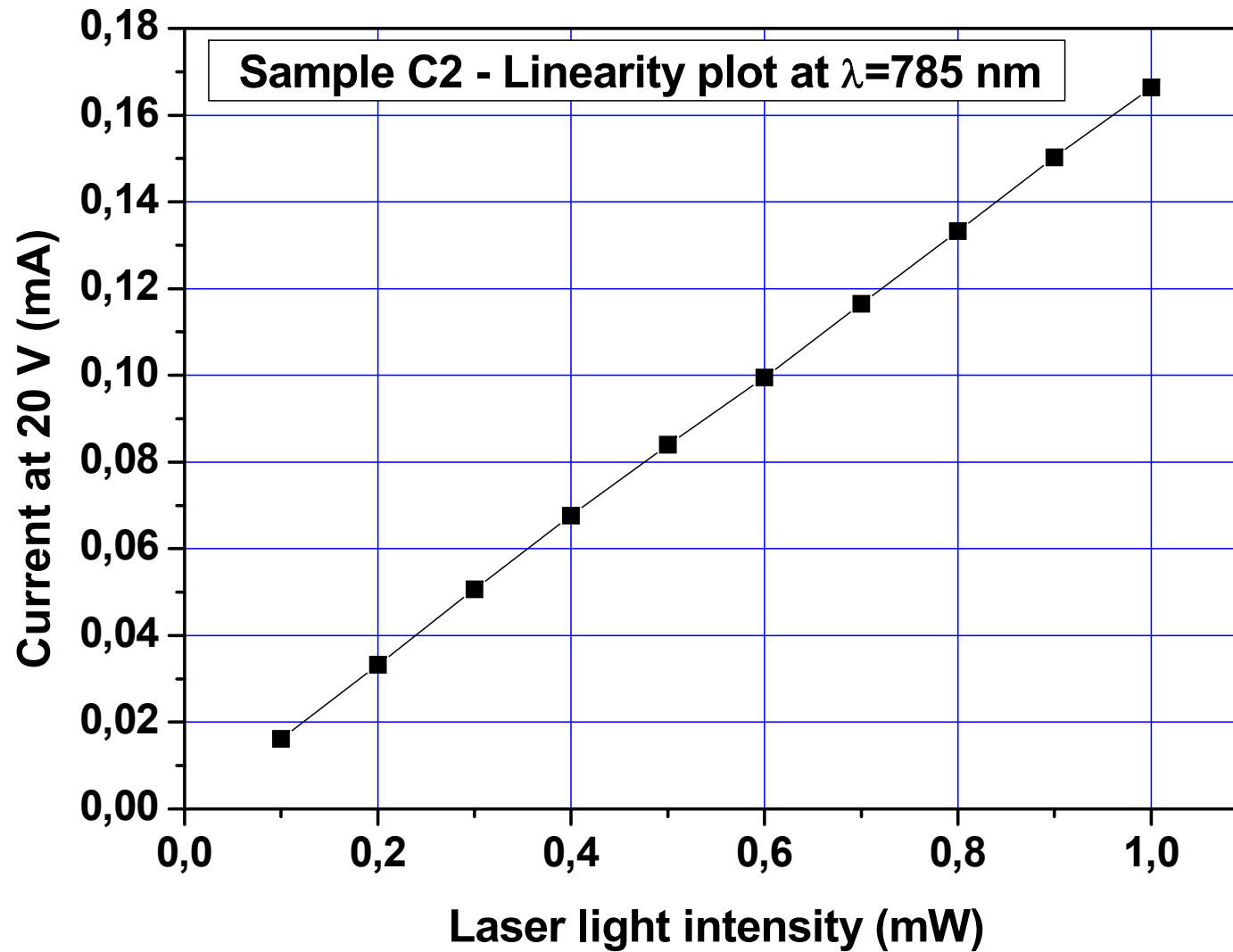
No saturation observed

No aging in two years

Uniformity on all the CNT surface

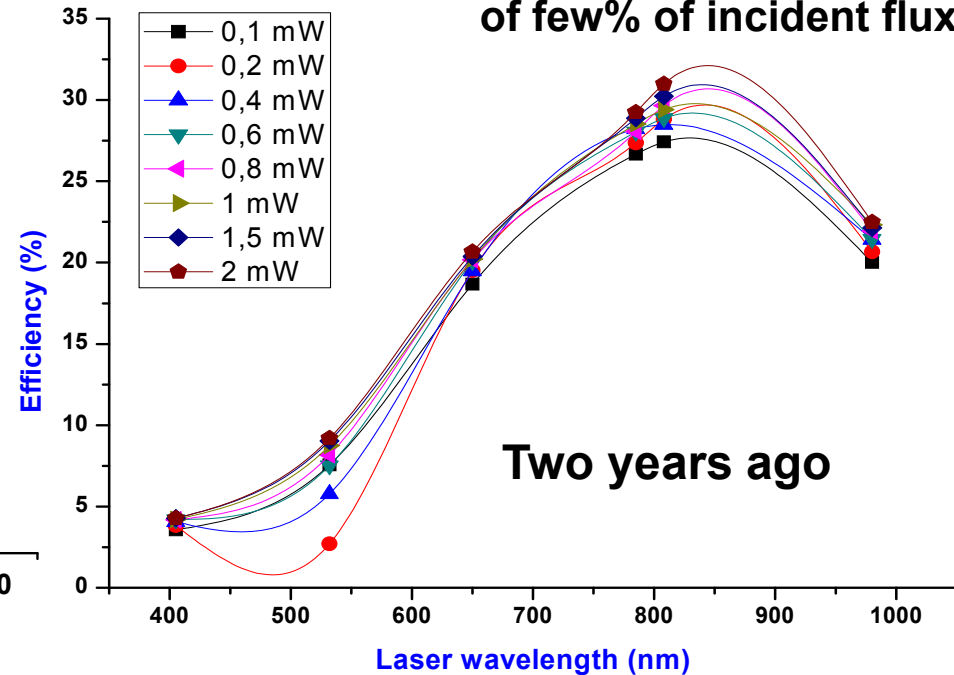
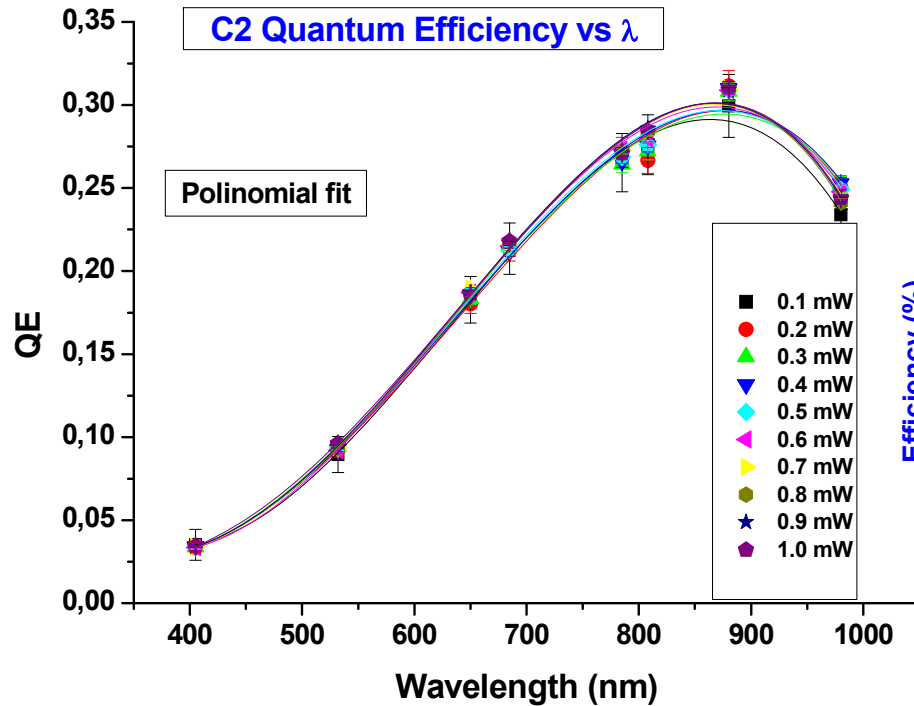
Breakdown @ >100 V

Photocurrent Linearity



Quantum Efficiency @ 25V

C2 detector



The amount of light reflected by surfaces is of few% of incident flux.

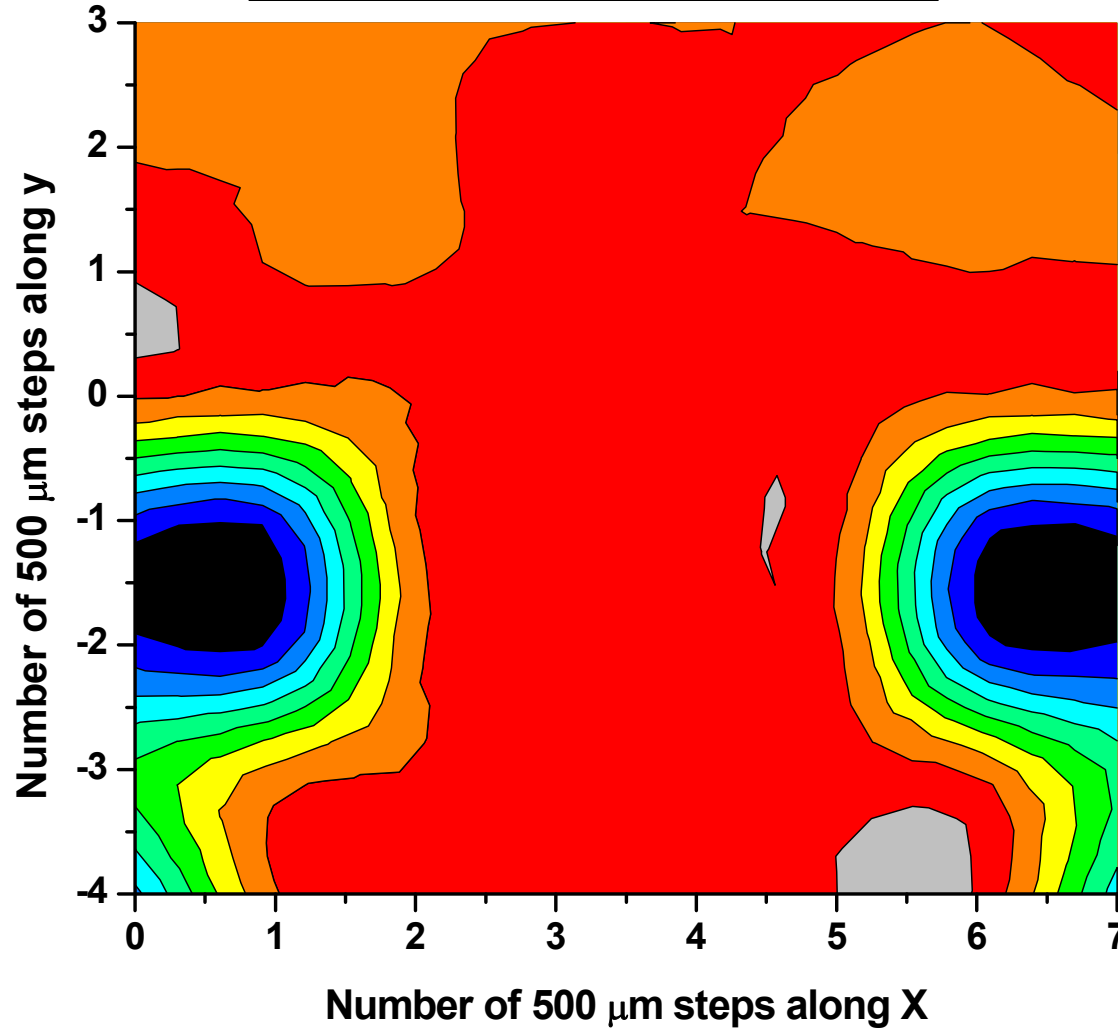
Two years ago

$$\eta = \frac{I_{sat} hc}{e P \lambda}$$

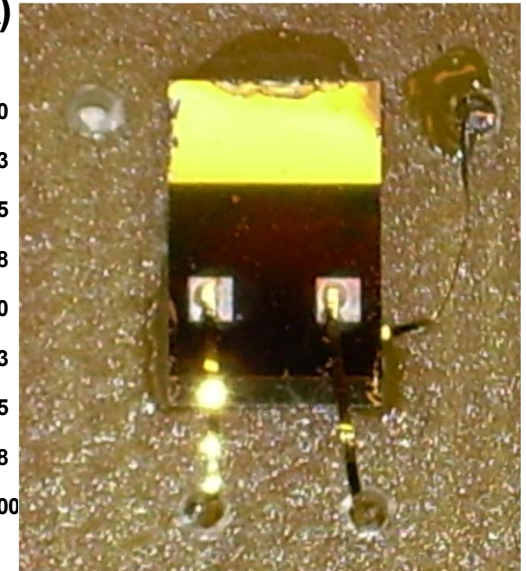
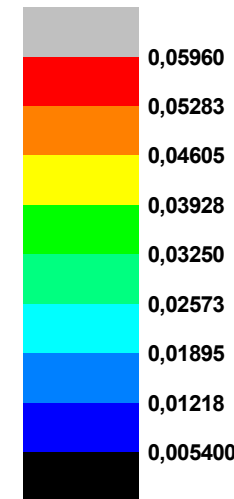
For each wavelength 20 measurements of photocurrent induced in the detector for various light intensities permit to estimate the mean value with combined errors of ratio between the number of drained charges and the number of incident photons.

Photocathode uniformity

Sample C2 - Photocurrent map

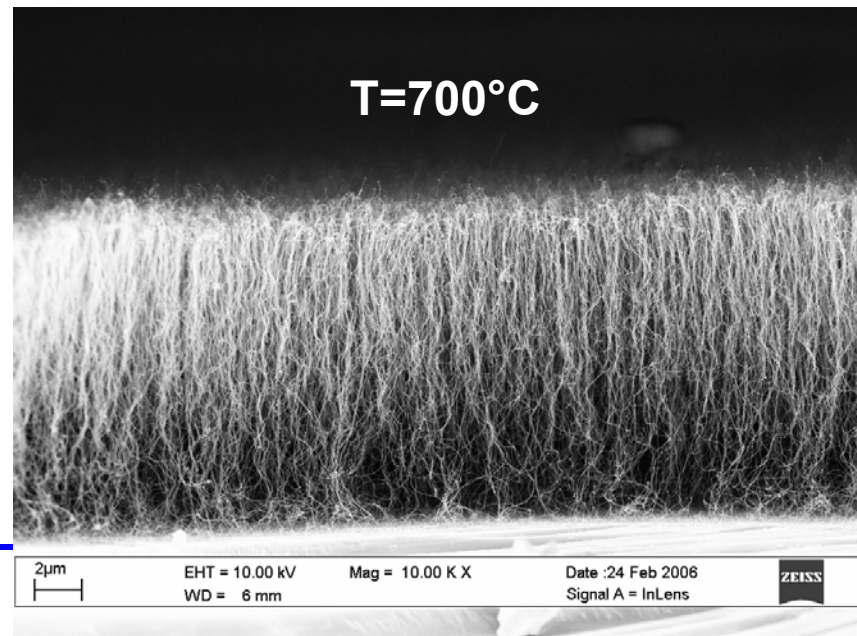
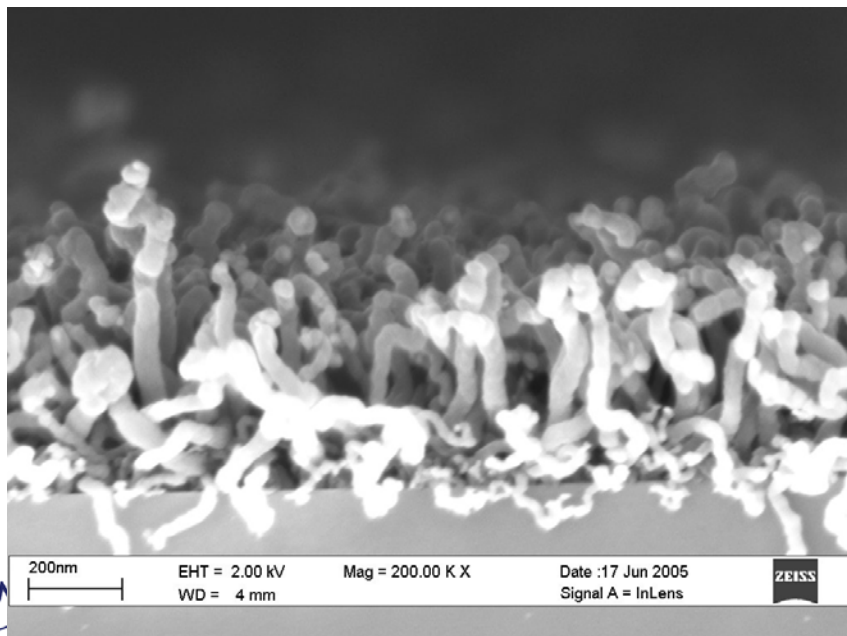
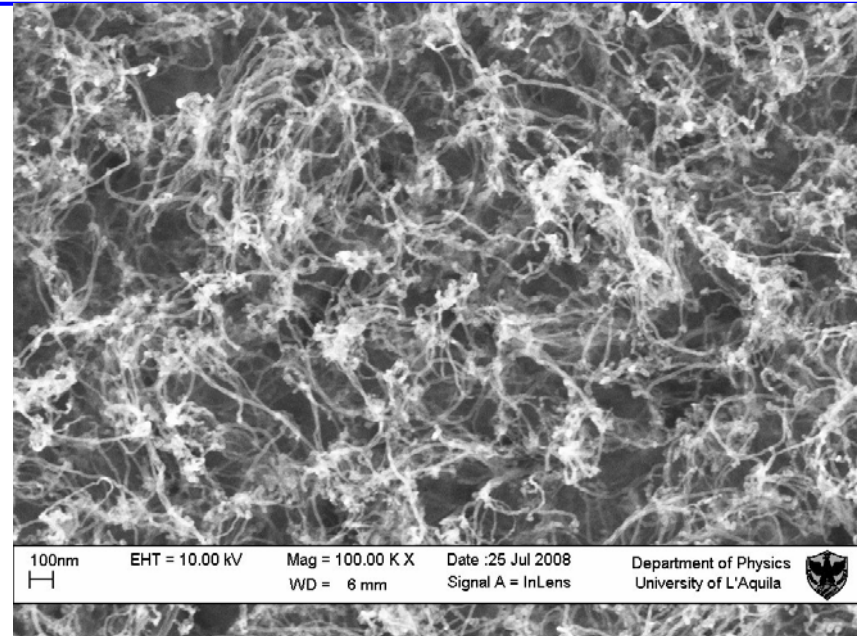
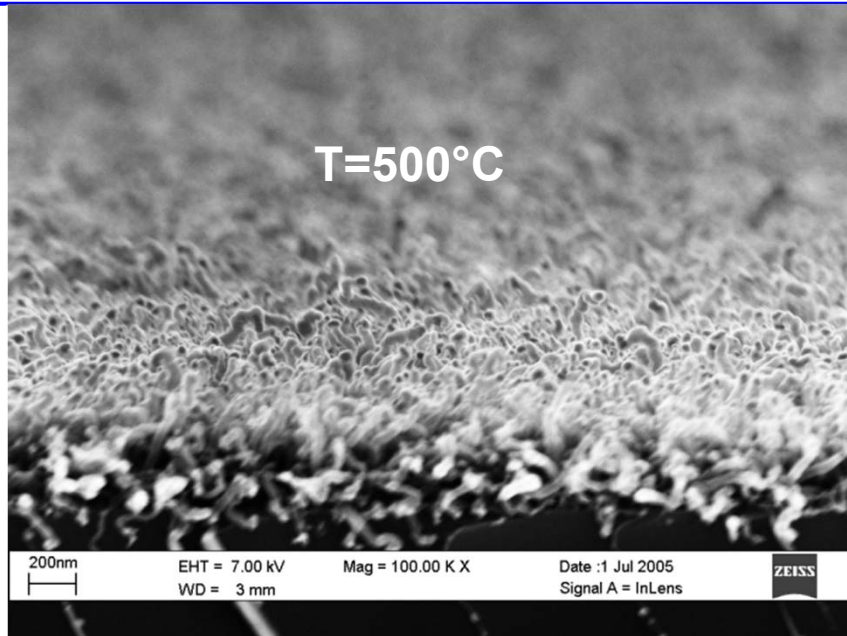


Current (mA)



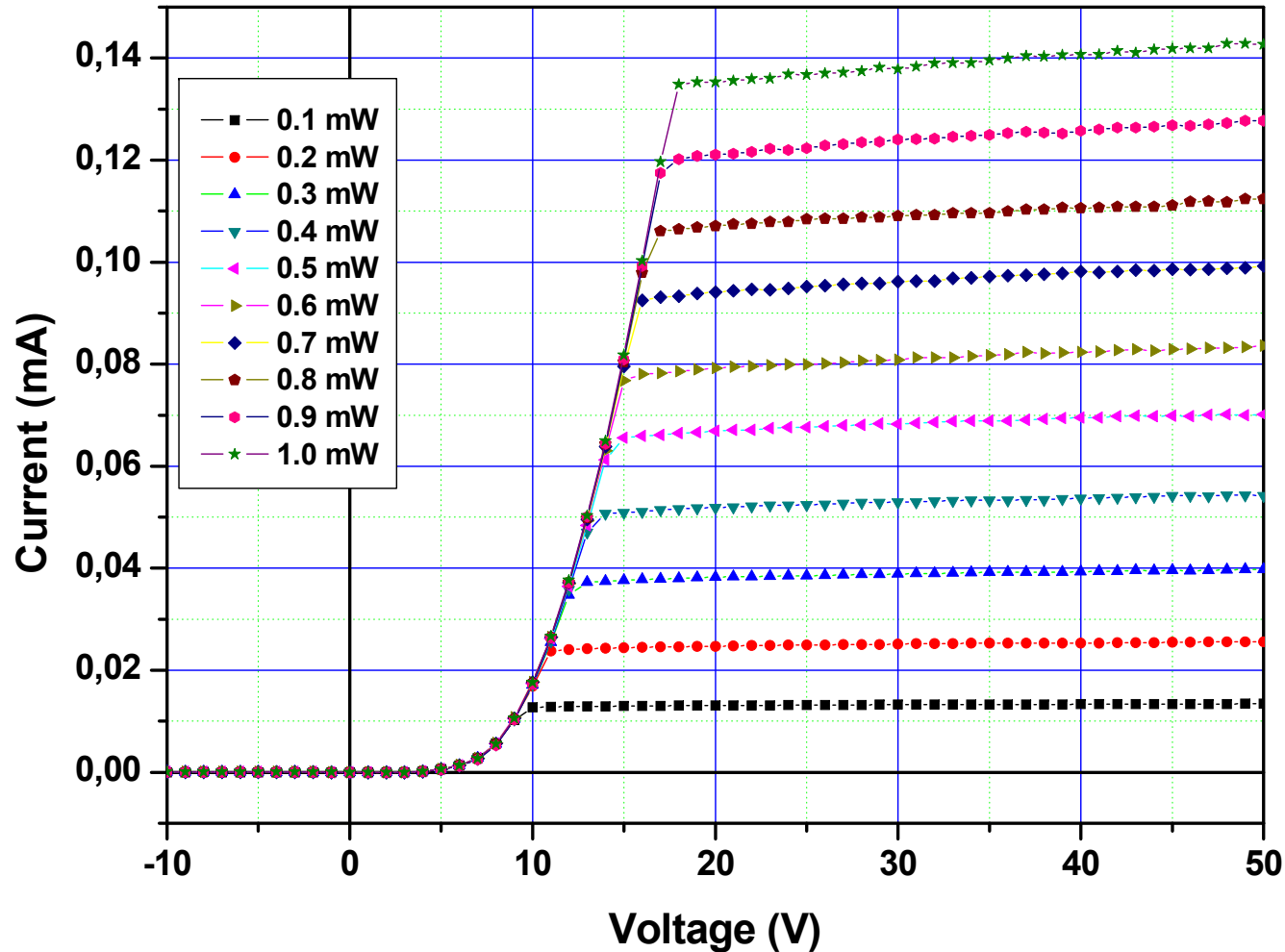
No signal appears illuminating the silicon substrate.

Comparison between CNT growth at 500 and 700 °C



700 °C - D detector @ $\lambda=650$ nm

Sample D - IV plot for various light intensities at $\lambda=650$ nm



Room temperature

No electronics

No signal amplification

Long and stable plateau

Linearity I vs W

Threshold 6.55 V

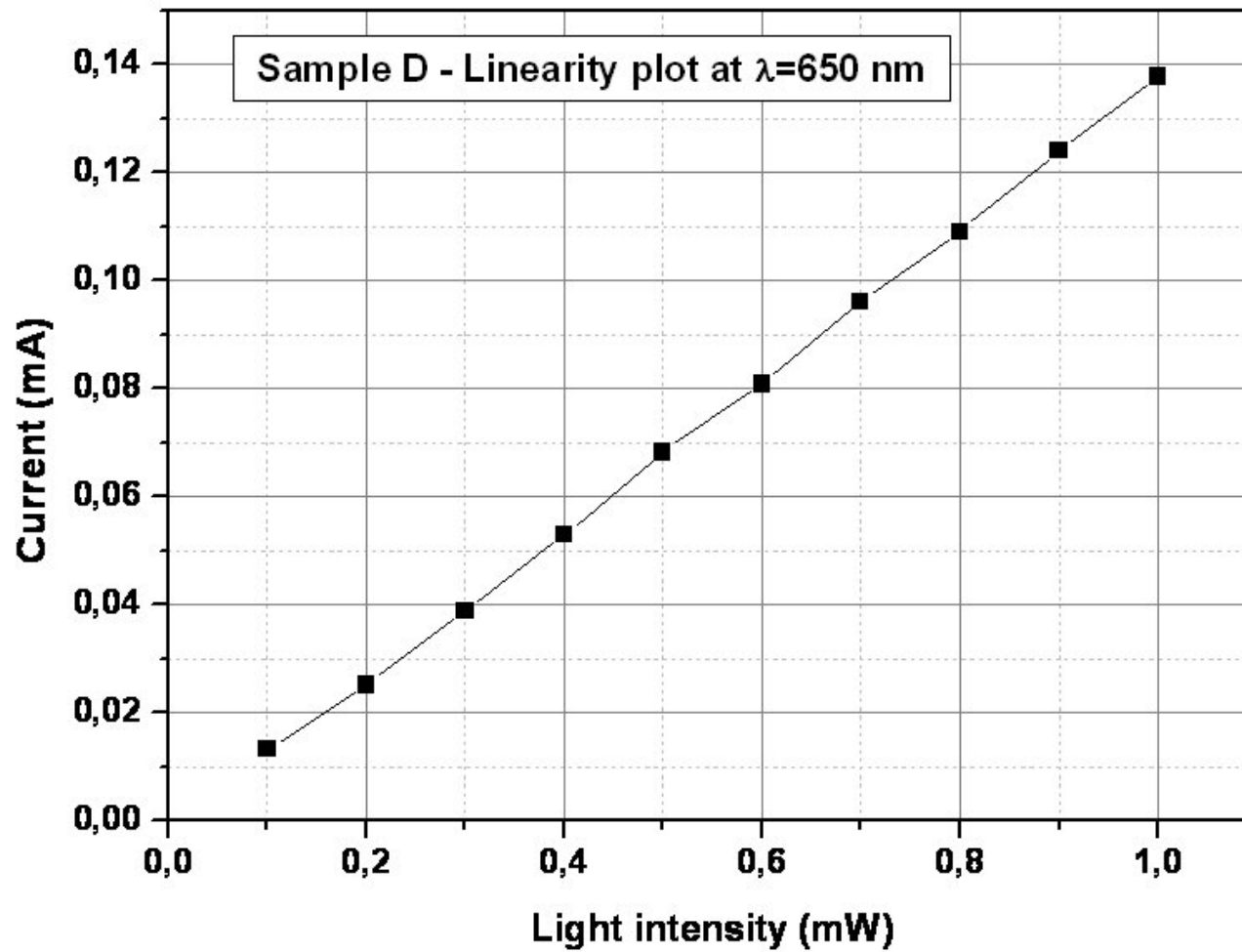
No saturation observed

No aging in two years

Uniformity on all the CNT surface

Breakdown @ >100 V

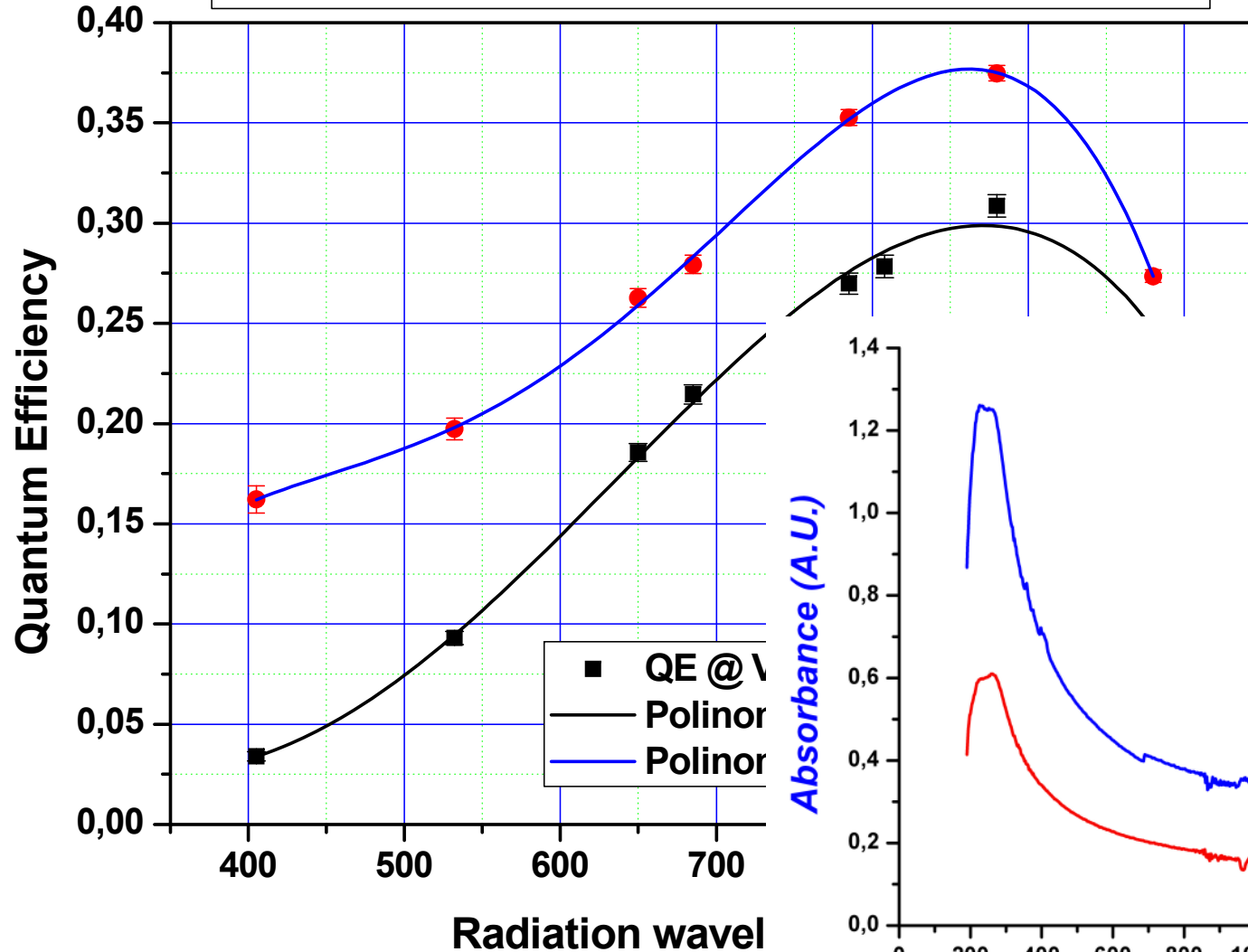
Photocurrent Linearity



QE

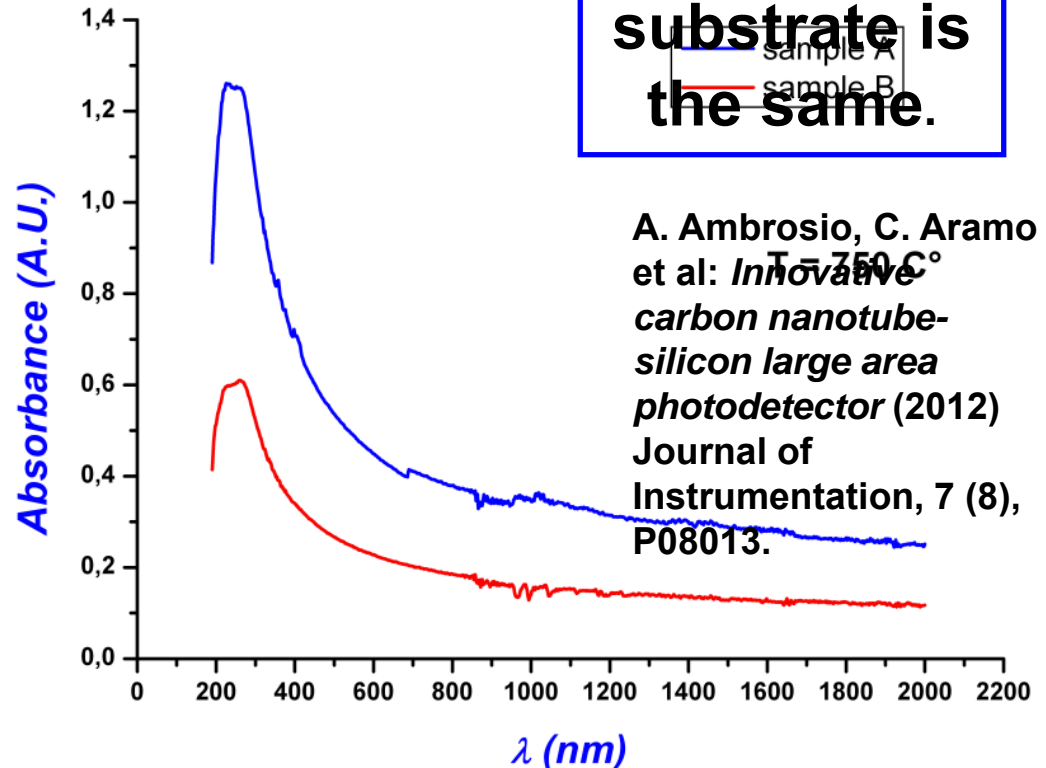
$$\eta = \frac{I_{sat} hc}{eP\lambda}$$

Comparison of quantum efficiency @ 500° and 700° C



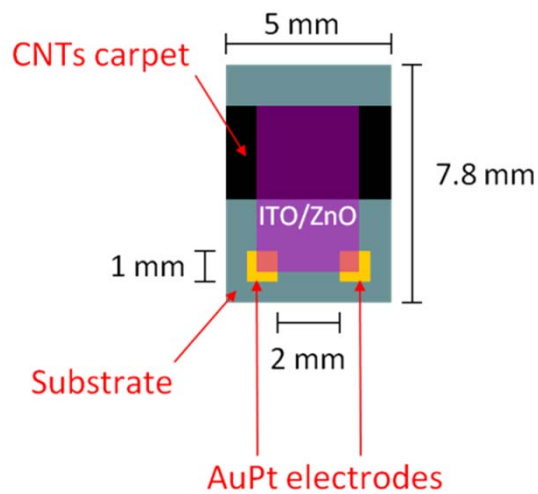
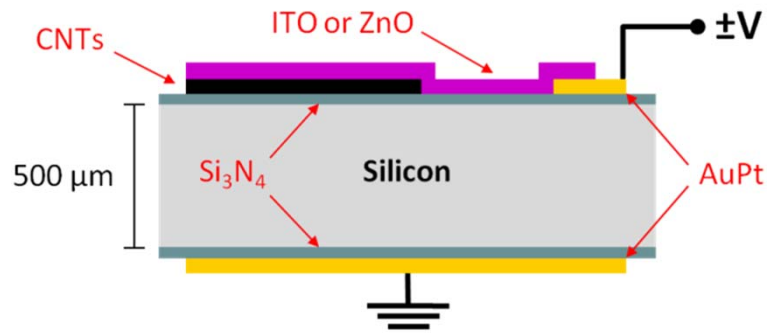
Higher T
↓
Higher UV photosensitivity

Note:
The silicon substrate is the same.



A. Ambrosio, C. Aramo et al: *Innovative carbon nanotube-silicon large area photodetector* (2012) Journal of Instrumentation, 7 (8), P08013.

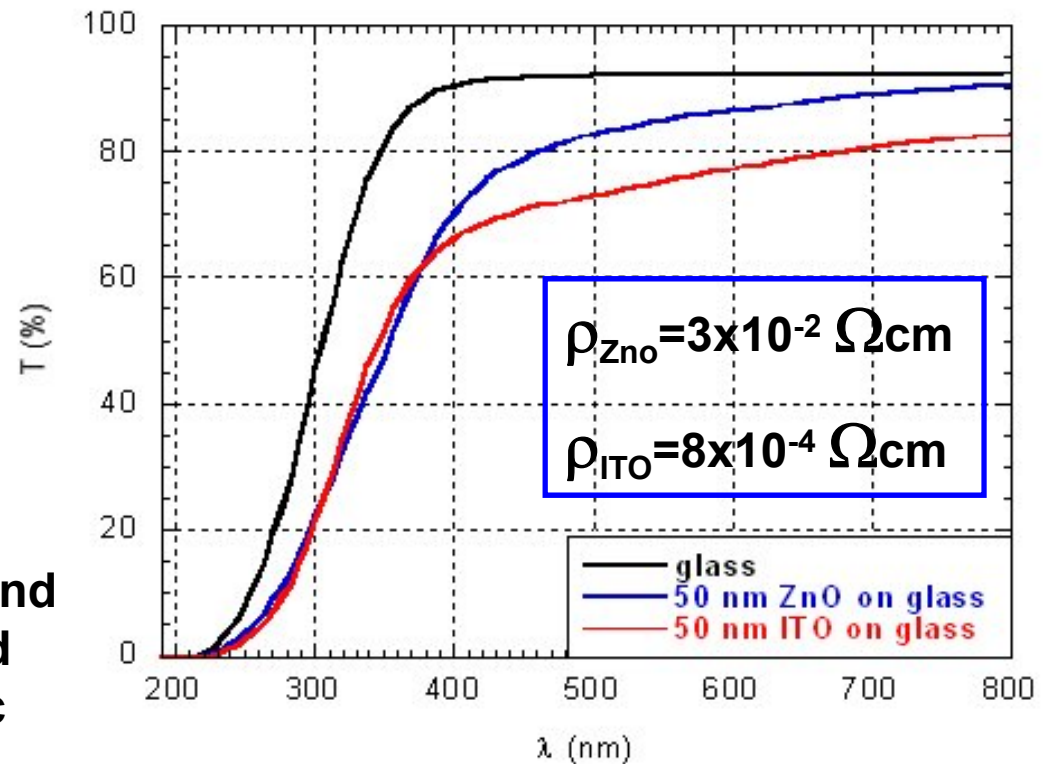
Coating - Sample IBS0955 @ 500°



(a)

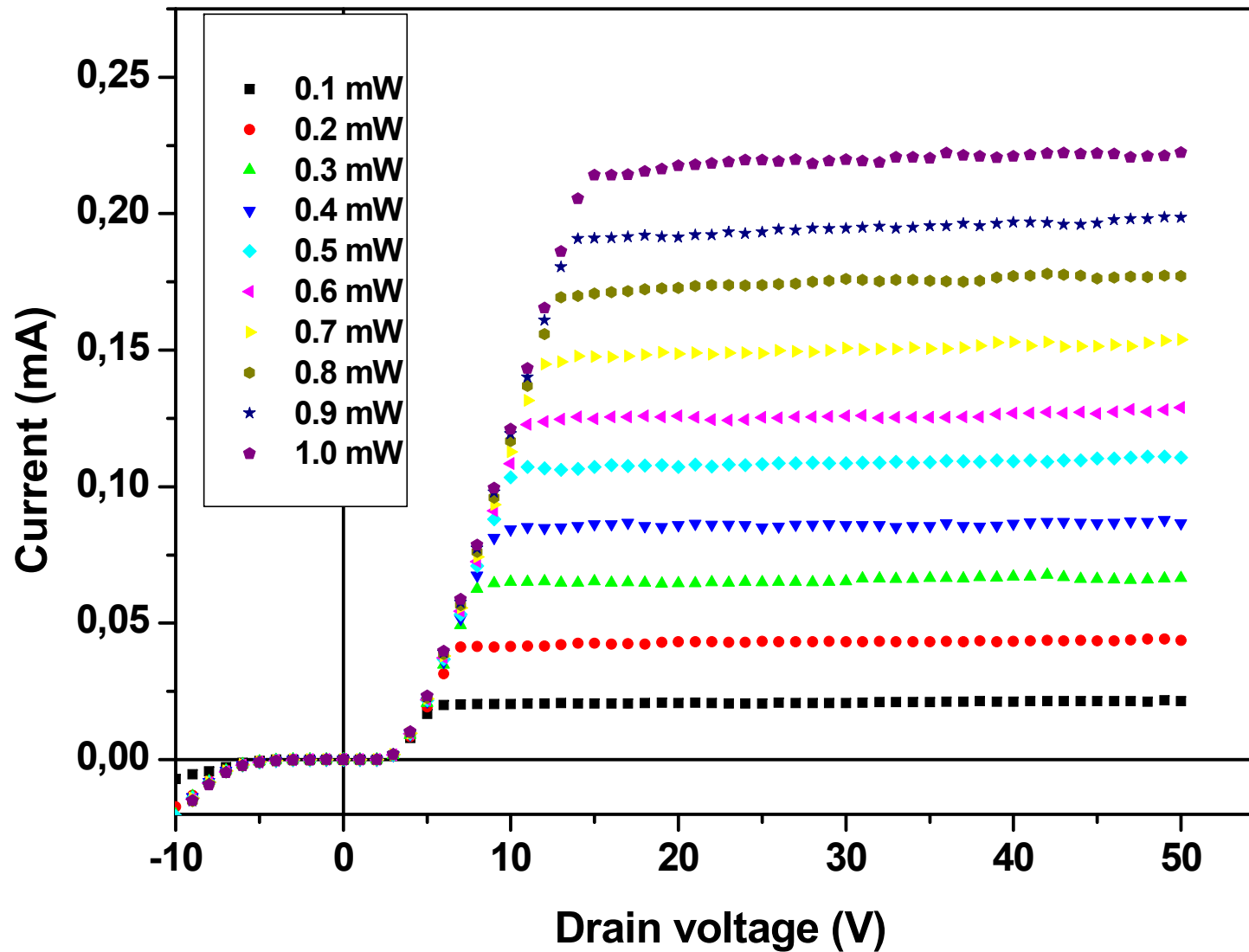
Optical properties of TCO films and their electrical resistivity ensured the formation of near ideal ohmic contact.

In order to obtain a CNTs coating, a thin film of a transparent conductive oxide (TCO), namely indium tin oxide (ITO) or zinc oxide (ZnO), is sputtered on the CNTs network so to partially cover the Au/Pt pads.

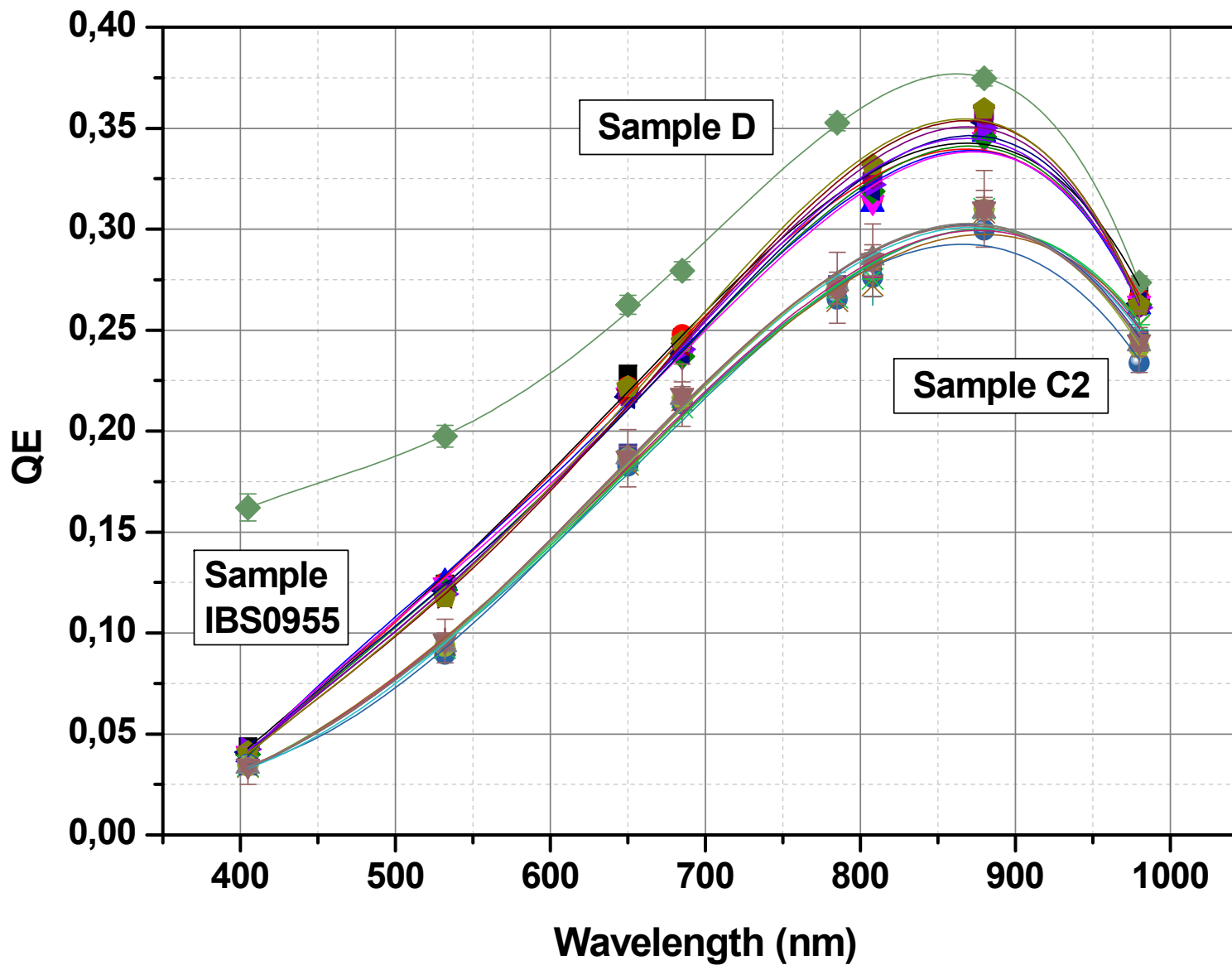


Sample ITO photocurrent

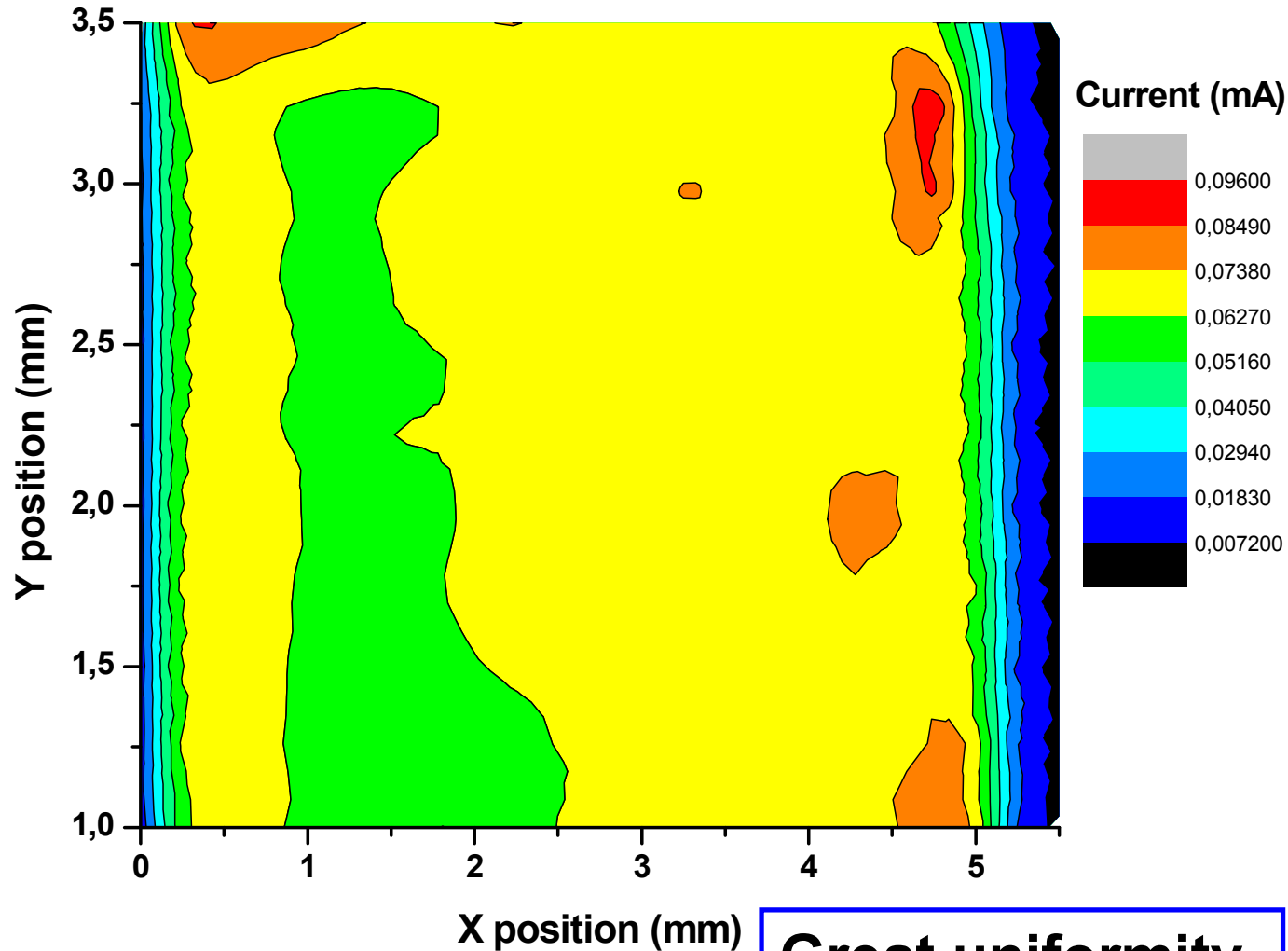
Sample IBS0955 with ITO - $\lambda=808$ nm



QE comparison for samples C2_500°, D_700° and IBS0955_500°



Map of sample IBS0955



**Great uniformity
over large area**

The electric field applied uniformly over the entire CNT surface plays a fundamental role making uniform the charge electrodes.

The signal generated everywhere in the sample can be collected to the metallic electrodes through the ITO layer, whose resistivity is very low.

Study of heterojunction Si-CNT



Contents lists available at ScienceDirect

Nuclear Instruments and Methods in Physics Research A

journal homepage: www.elsevier.com/locate/nima



Electrical analysis of carbon nanostructures/silicon heterojunctions designed for radiation detection

A. Tinti^{a,*}, F. Righetti^a, T. Ligonzo^a, A. Valentini^a, E. Nappi^a, A. Ambrosio^b, M. Ambrosio^c, C. Aramo^c, P. Maddalena^b, P. Castrucci^d, M. Scarselli^d, M. De Crescenzi^d, E. Fiandrini^e, V. Grossi^f, S. Santucci^f, M. Passacantando^f

^a INFN, Sezione di Bari, Via Amendola 173, 70126 Bari, Italy

^b CNR-SPIN U.O.S. di Napoli e Dipartimento di Scienze Fisiche, Università degli Studi di Napoli Federico II, Via Cintia 2, 80126 Napoli, Italy

^c INFN, Sezione di Napoli, Via Cintia 2, 80125 Napoli, Italy

^d Dipartimento di Fisica, Università degli Studi di Roma Tor Vergata, Via della Ricerca Scientifica 1, 00133 Roma, Italy

^e INFN, Sezione di Perugia e Dipartimento di Fisica, Università degli Studi di Perugia, Piazza Università 1, 06100 Perugia, Italy

^f Dipartimento di Fisica, Università degli Studi dell'Aquila, Via Vetoio 10, 67100 Coppito, L'Aquila, Italy

**Nuclear Instruments
and Methods in
Physics Research A
629 (2011), 377-381**

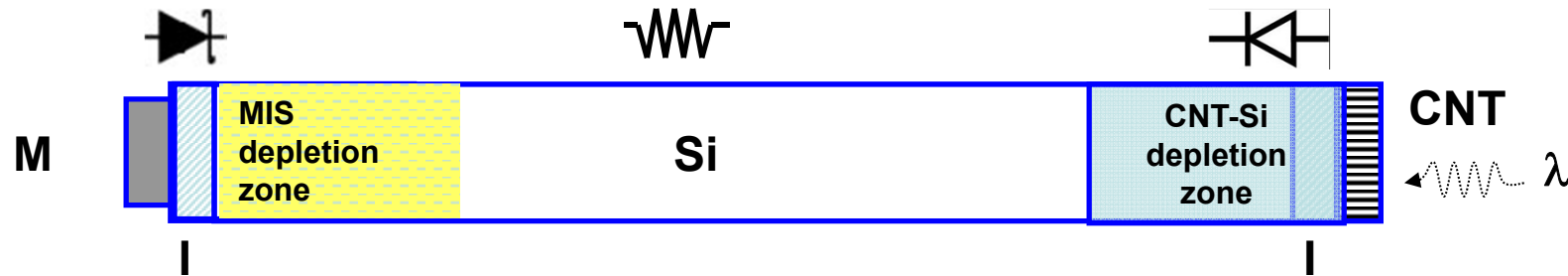
A B S T R A C T

A new class of radiation detectors based on carbon nanostructures as the active photosensitive element has been recently developed. In this scenario the optimization of the device, both in dark and on light irradiation, is a crucial point. Here, we report on electrical measurements performed in dark conditions on carbon nanofibers and nanotubes deposited on silicon substrates. Our experimental results were interpreted in terms of a multistep tunneling process occurring at the carbon nanostructures/silicon interface.

Keywords:
Carbon nanotubes

© 2010 Elsevier B.V. All rights reserved.

Device configuration



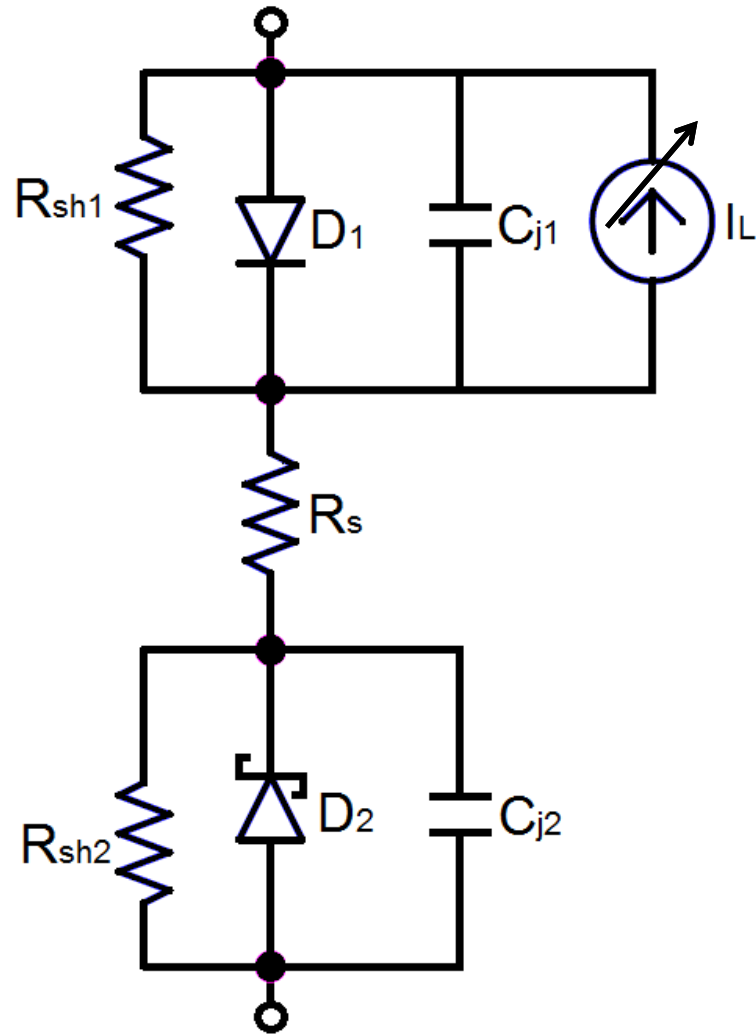
Depletion regions depend on applied voltage. The silicon bulk, 500 μm thick, can be considered as a passive resistance except in the depletion areas.

The MIS depletion zone cannot be reached from optical radiation because of the presence of metal.

Instead the depletion area created by the heterojunction CNT-Si can be reached and activated by radiation due to the characteristics of nanotubes. A fraction is absorbed inside CNT and converted in hole-electron pairs or excitons. The other reached silicon and is converted inside.

The described device can be considered as a “**phototransistor**”

Equivalent circuit



I_L : photocurrent generated from incident radiation

C_j : Junction capacity

R_{sh} : Shunt resistance

R_s : Resistance

D_1 : CNT-Si heterojunction

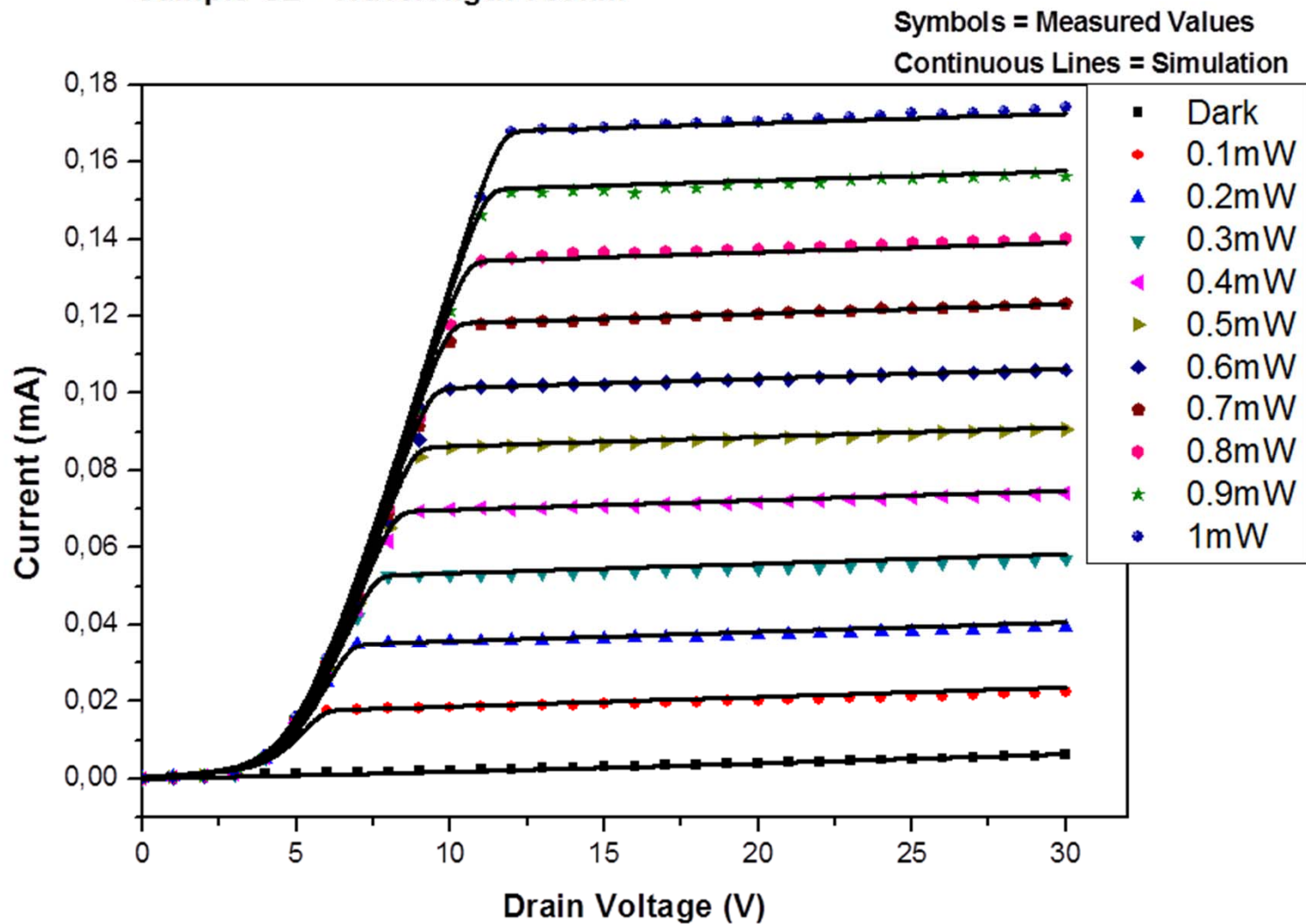
D_2 : MIS tunnel junction

In order to simulate the device we used the *PSpice Model Editor*

Comparison with simulation

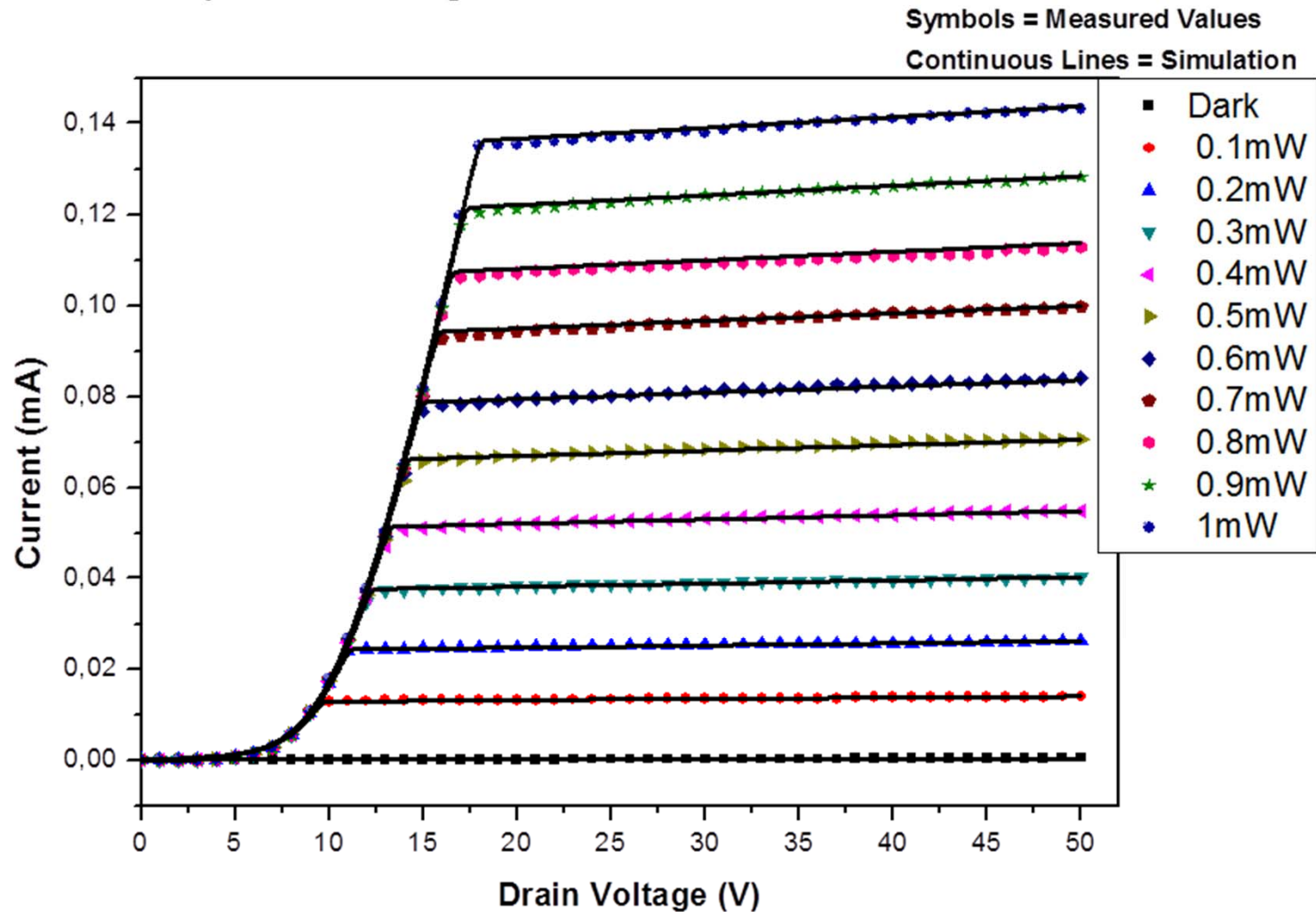
sample C2 – 500 °C

Sample C2 - Wavelength 785nm



Comparison with simulation sample D – 700 °C

Sample D - Wavelength 650nm



Other advantage

The new Si-CNT detector can offer another advantage: the possibility to pixel large area in a very cheap and easy way.

$$\frac{d^2 I}{d\Omega d\omega} = \frac{3\sigma_z}{4c\pi\sqrt{\pi}} P_0 \frac{1}{\gamma^4 \theta^4} \exp\left(\frac{-\omega^2 \theta^4 \sigma_z^2}{16c^2}\right)$$

The angular intensity distribution depends from wavelength as power 2 whereas the dependence from angle as power 4: two order of magnitude higher!

This means that with pixelled detector it will be possible to apply the LABM with higher sensitivity.

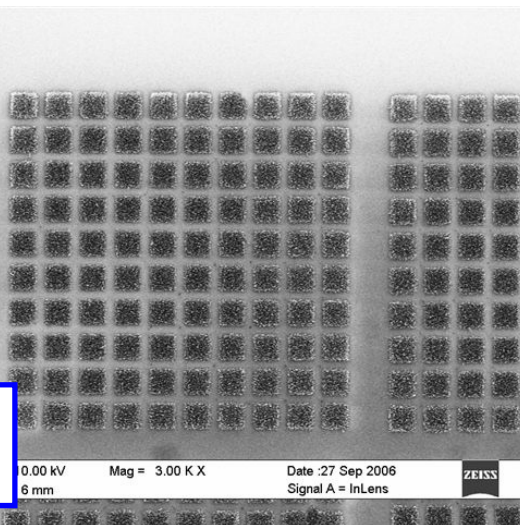
Nano-pixelled photocathodes

MWCNTs can be grown on different kind of substrates according the desired geometry. Nanolithography process allows to obtain finely pixelled elements over large surfaces.

10 x 10
pixel
CNT

4 μm per
cell

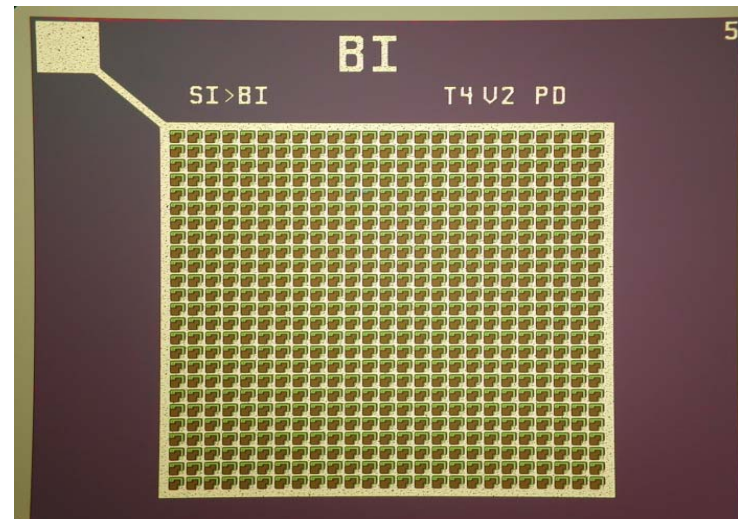
0.05 x 0.05
 mm^2 dimension



25 x 25
pixel
SiPM

40 μm
per cell

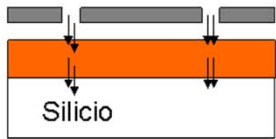
1 x 1 mm^2
dimension



Nano-pixelled photocathodes may be obtained by means of nanolithography in a very cheap and easy way!

Nanolithography and patternization

Electron beam exposure



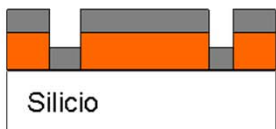
GDSII mask design



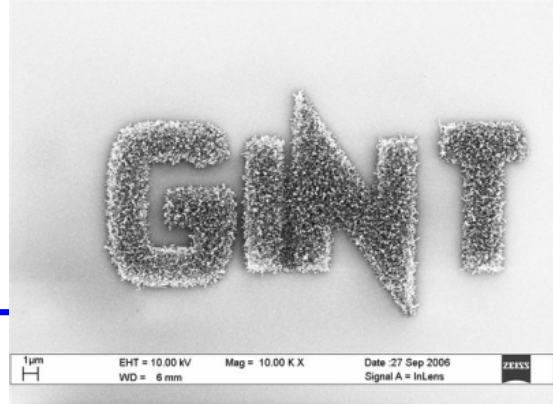
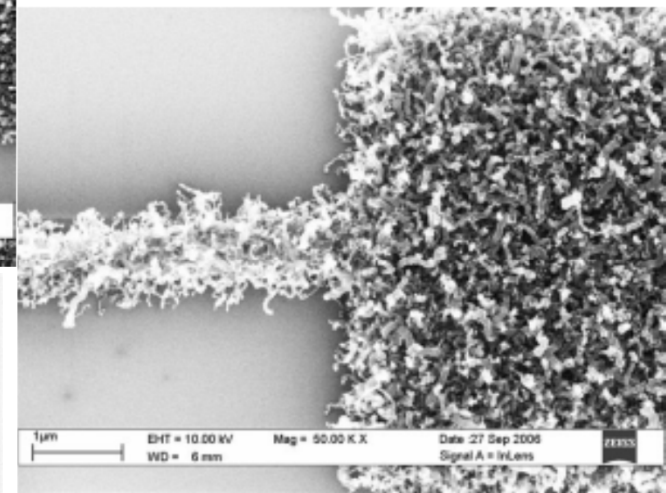
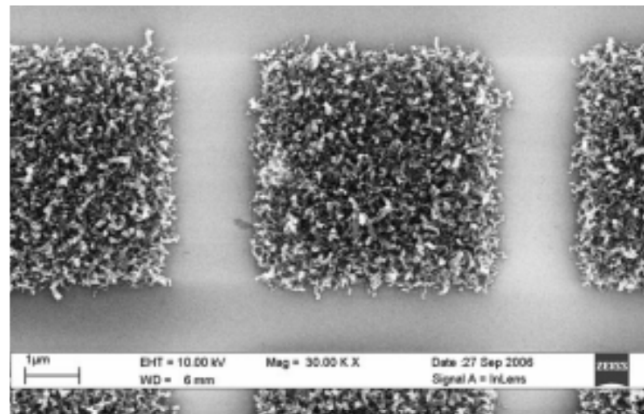
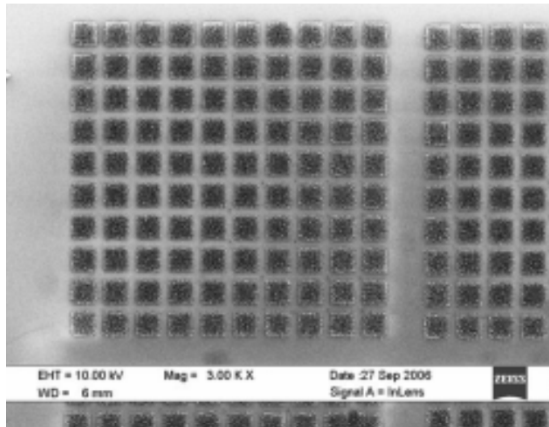
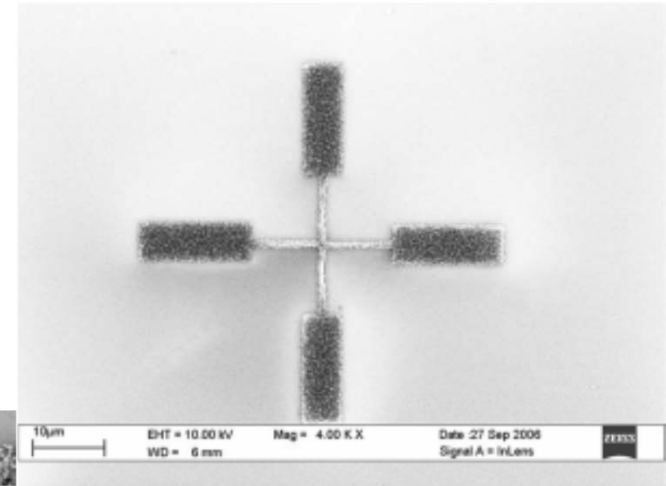
After developing



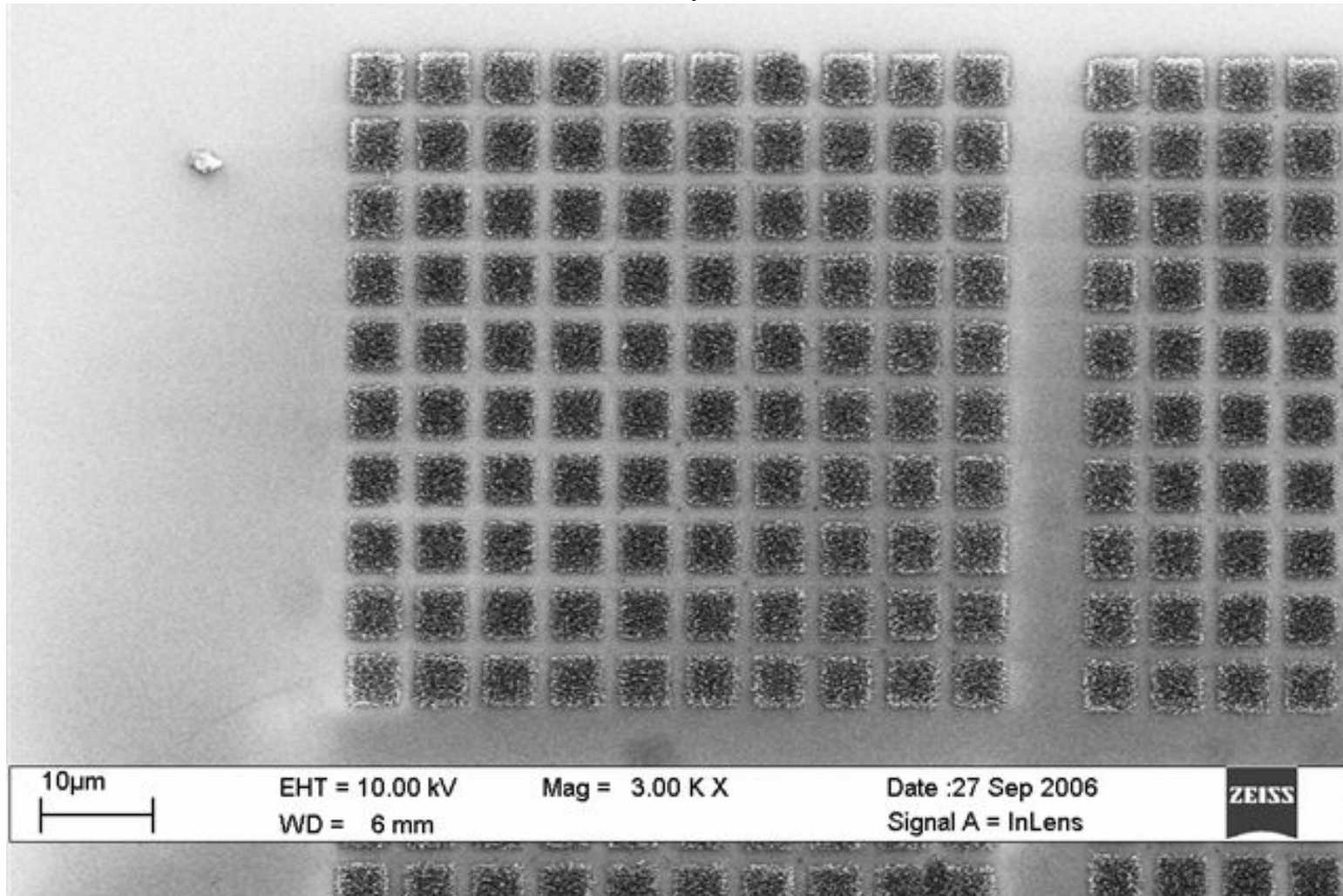
Nichel film deposition

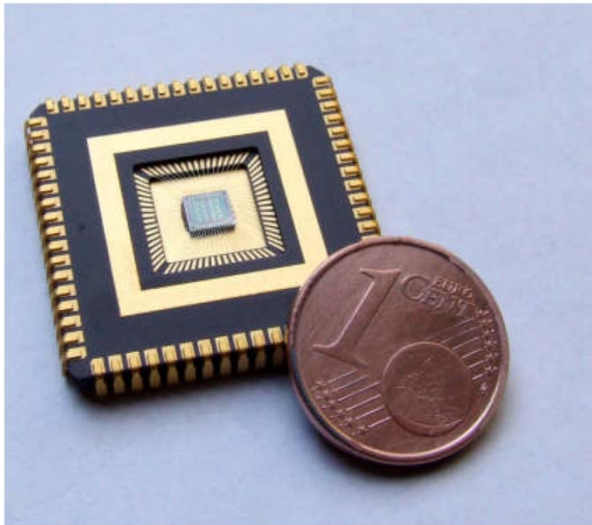


Aceton bath



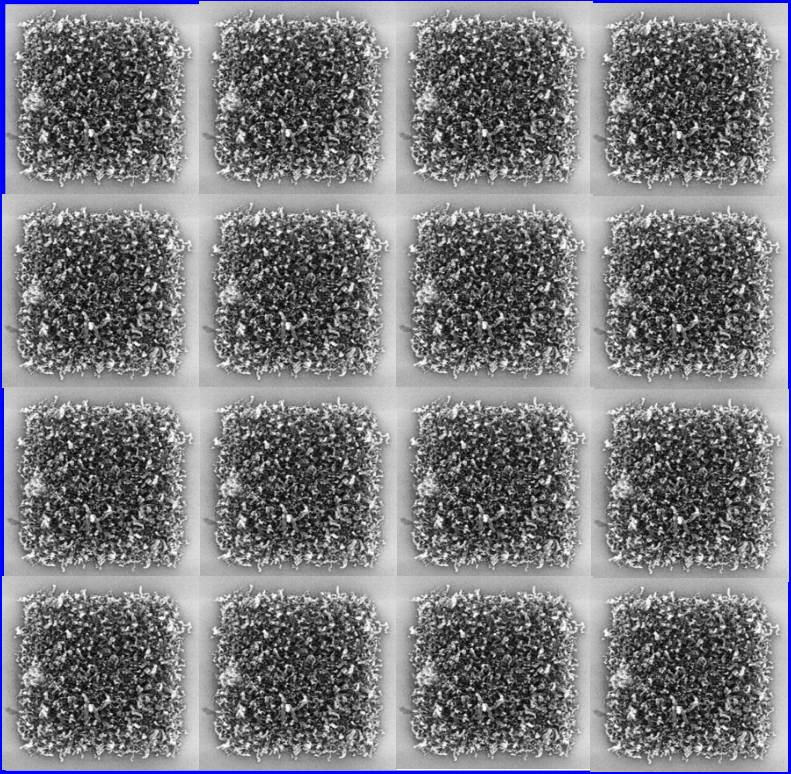
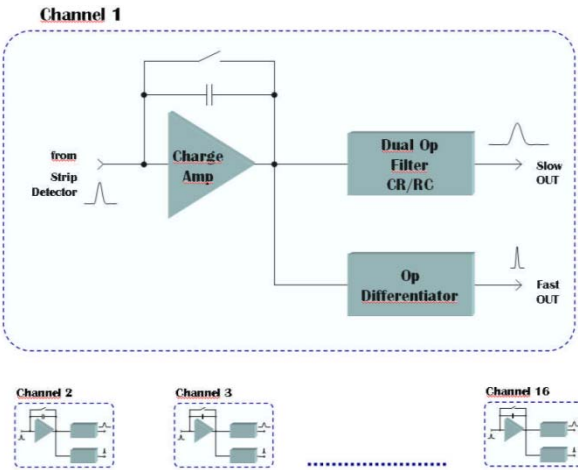
$$\frac{d^2 I}{d\Omega d\omega} = \frac{3\sigma_z}{4c\pi\sqrt{\pi}} P_0 \frac{1}{\gamma^4 \theta^4} \exp\left(\frac{-\omega^2 \theta^4 \sigma_z^2}{16c^2}\right)$$





A possible layout for a beamstrahlung photodetector

Analog chip MAGMA developed in Naples



1 cm² photodetector

8 pixel

Coating with ITO

Analog readout for each pixel

16 readout channels for each unit

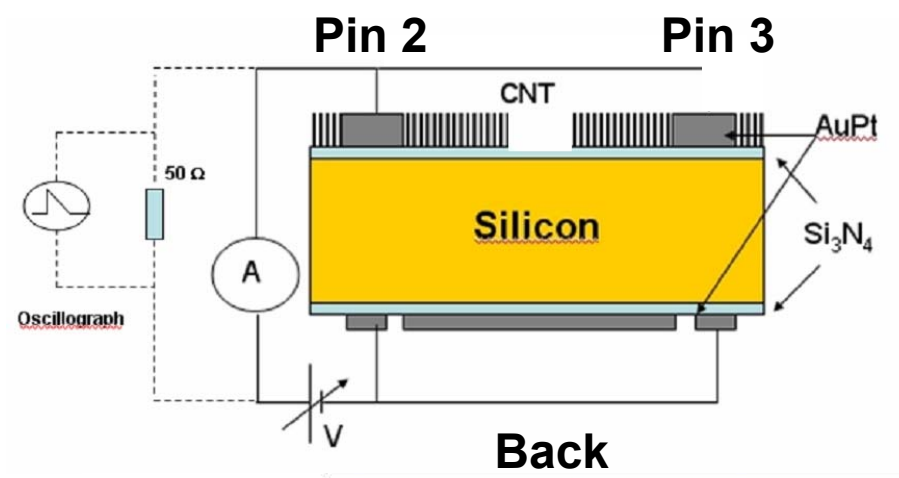
Reconstruct the beam shape at each frequency

Note: pixel dimensions are arbitrary. They depend on the light intensity and cost for pixel analog readout.

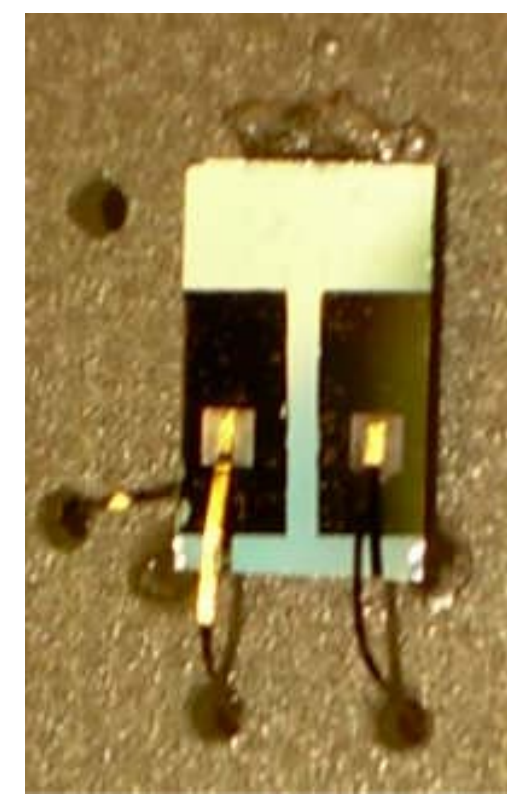
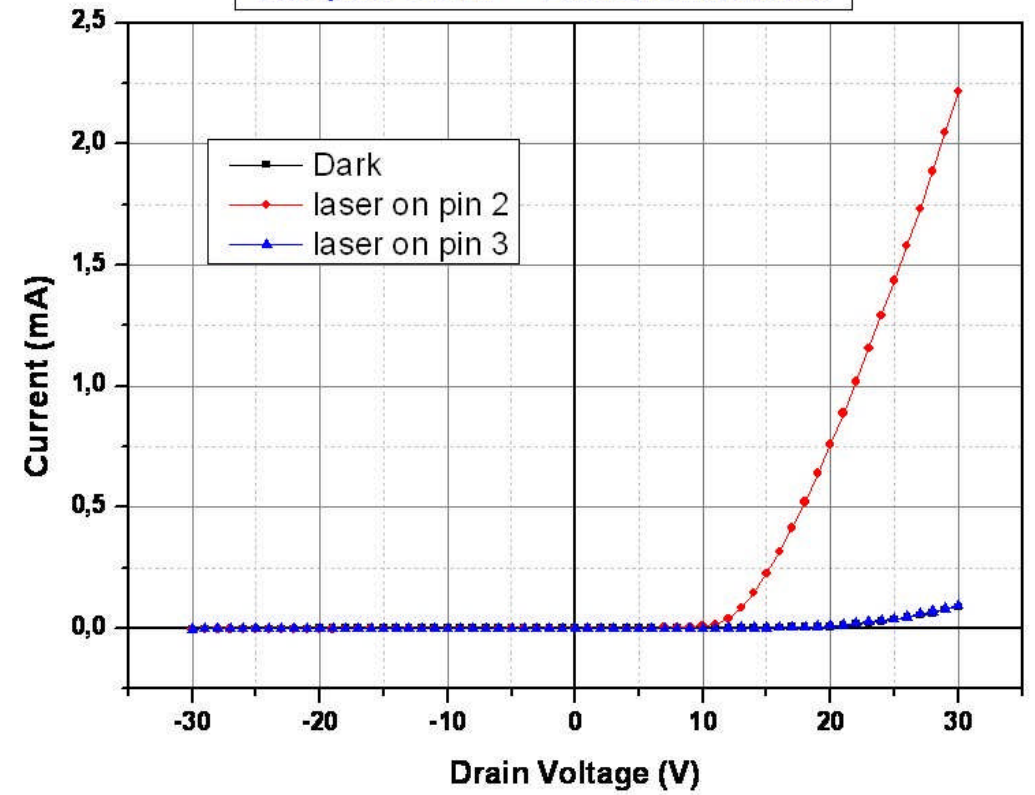
As higher is the pixel number as precise the reconstruction of beam shape.

Two insulae sample

$\lambda = 650 \text{ nm}$



Two pixel SiCNT - Back&front readout



Summary

A novel photon detector made of Silicon and CNT has been realized .

The main characteristics of this detector are:

- Low threshold
- Low dark current
- Large plateau region
- High linearity
- Stable at room temperature
- Quantum efficiency depending from light wavelength and from CVD temperature

Large area for large photocathodes

Easy pixellization

Sub-micrometer dimension of pixels

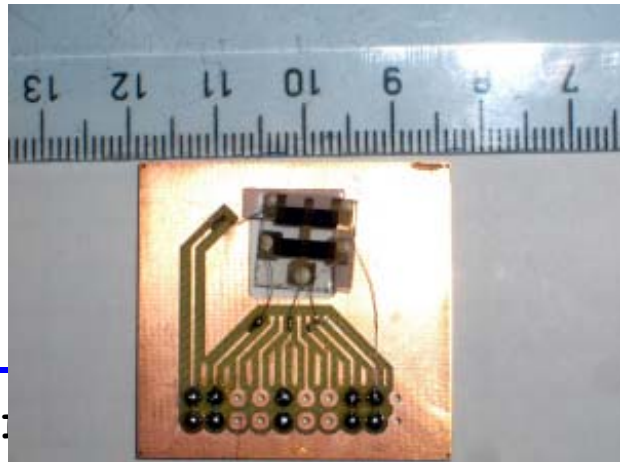
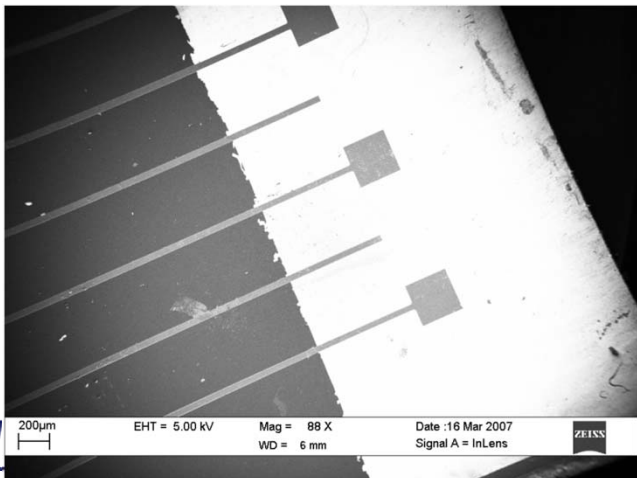
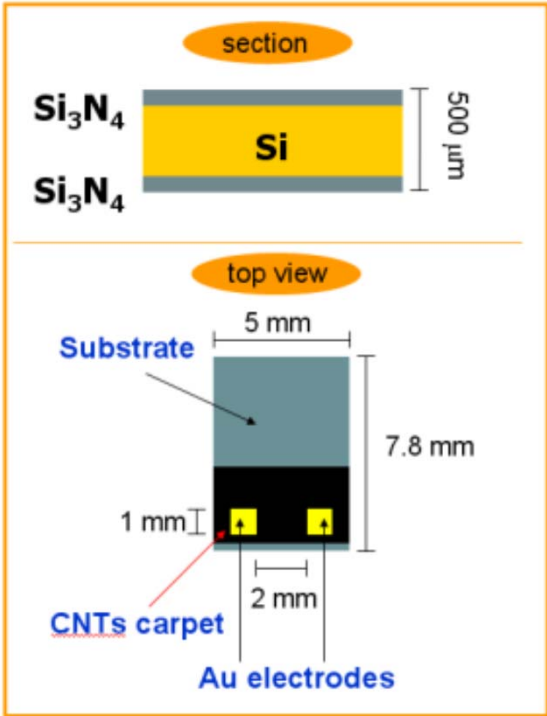
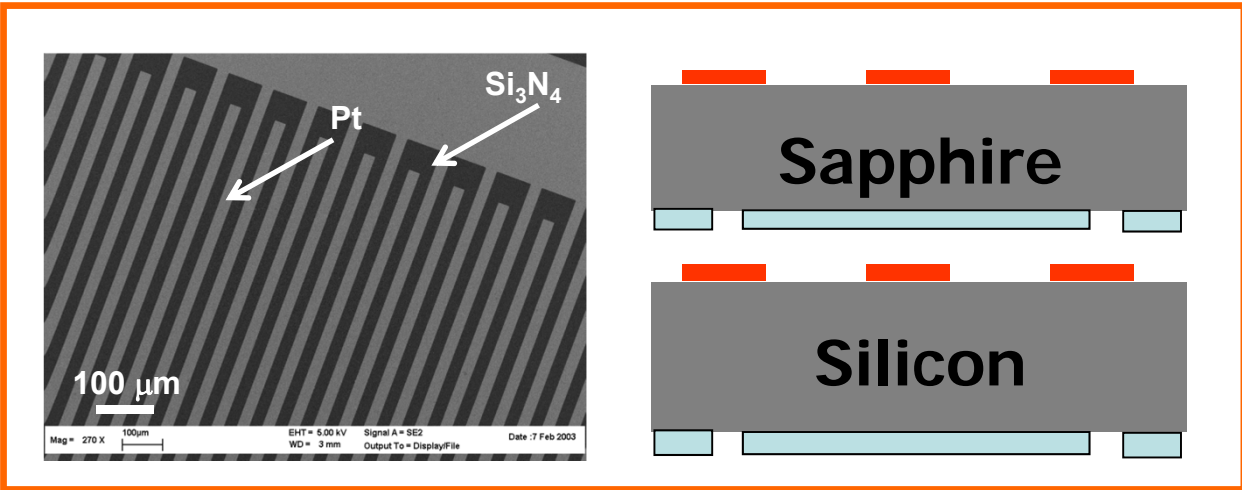
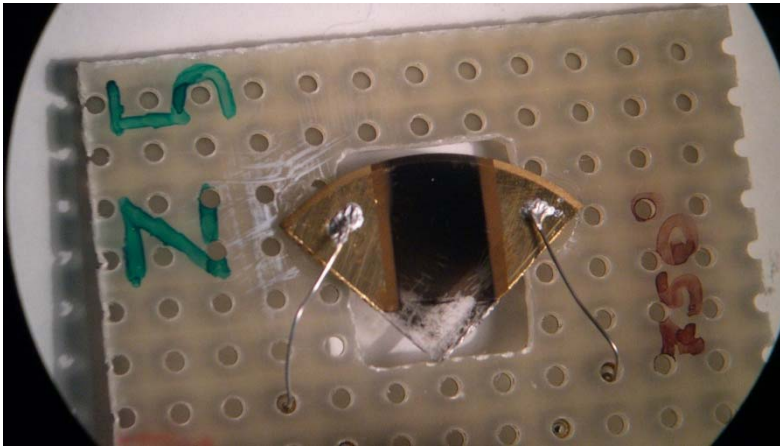
Coating of CNTs surface has been obtained with a conductive layer of ITO.
Detector aging is under investigation.

The possibility to use a detector with the described characteristics for the large angle beamstrahlung monitor permits to avoid different kind of photodetectors for different wavelength range and to improve two order of magnitude the sensitivity of the method.

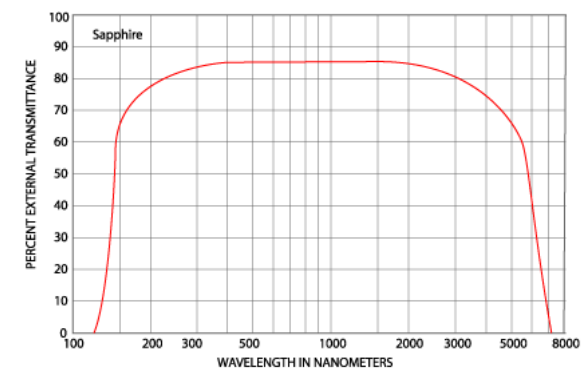
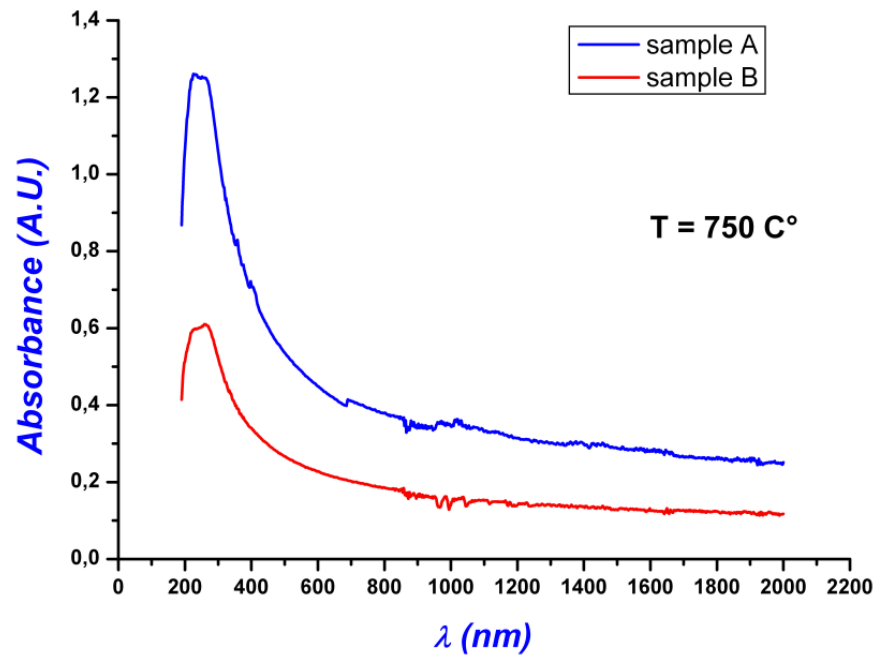
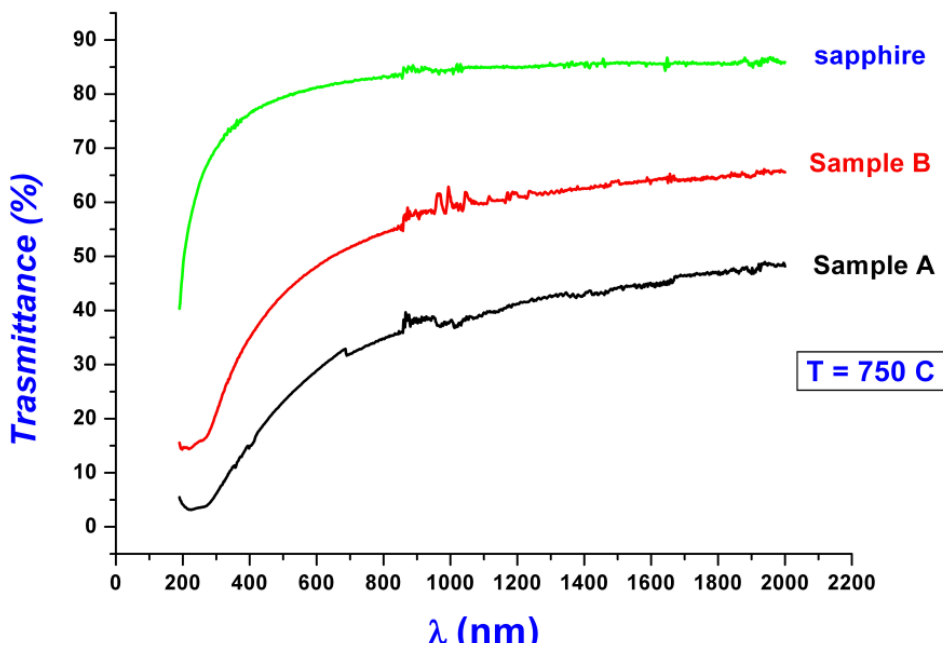


LFF Workshop - Napoli - November, 22-23 2012

Thank you for attention

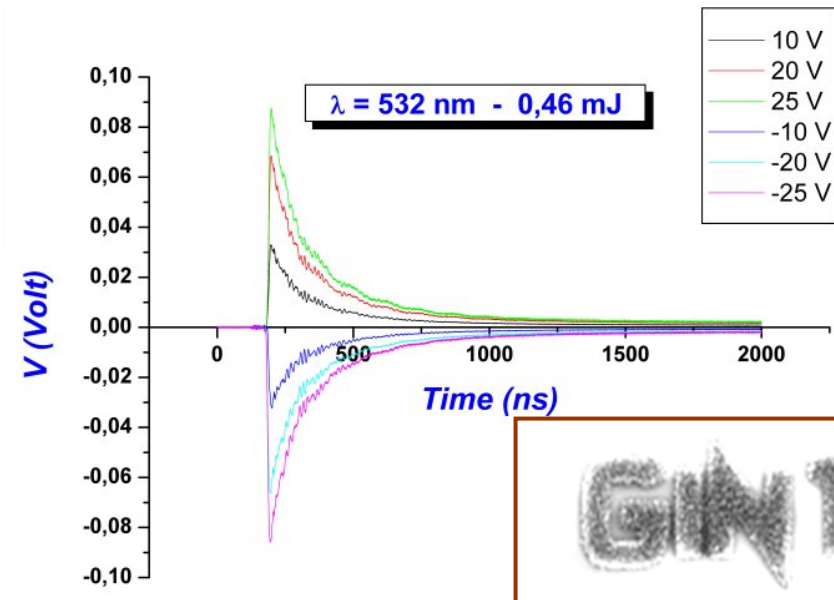
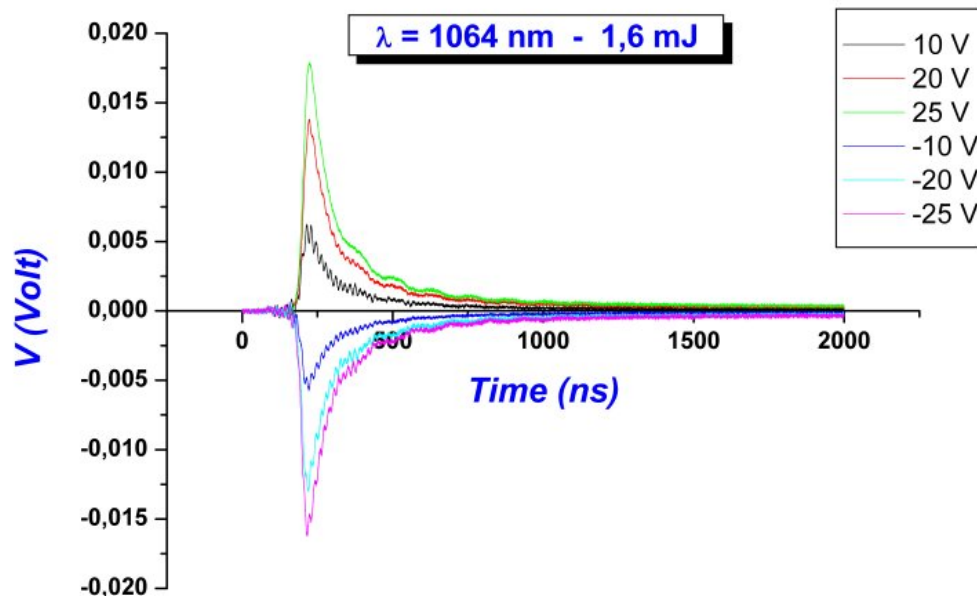
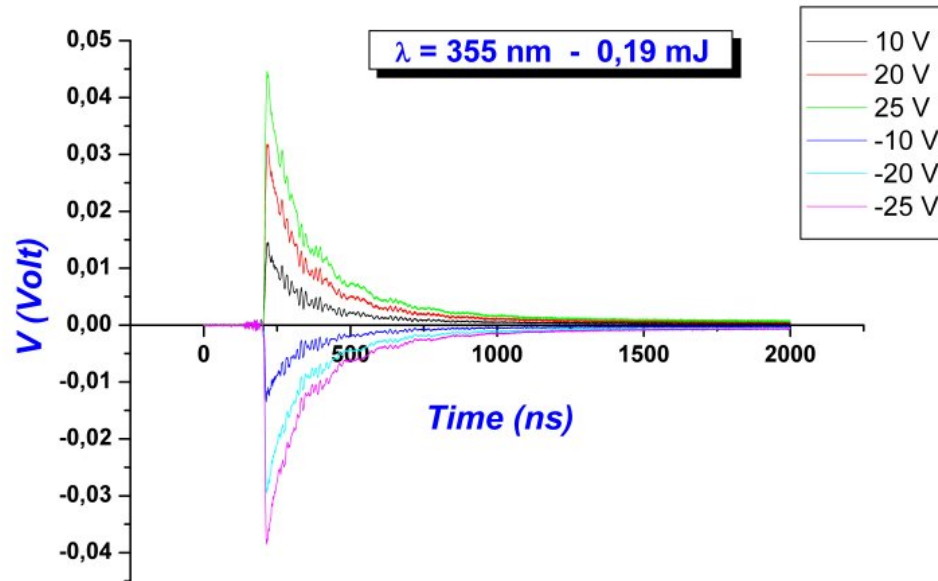


Various kind of substrates



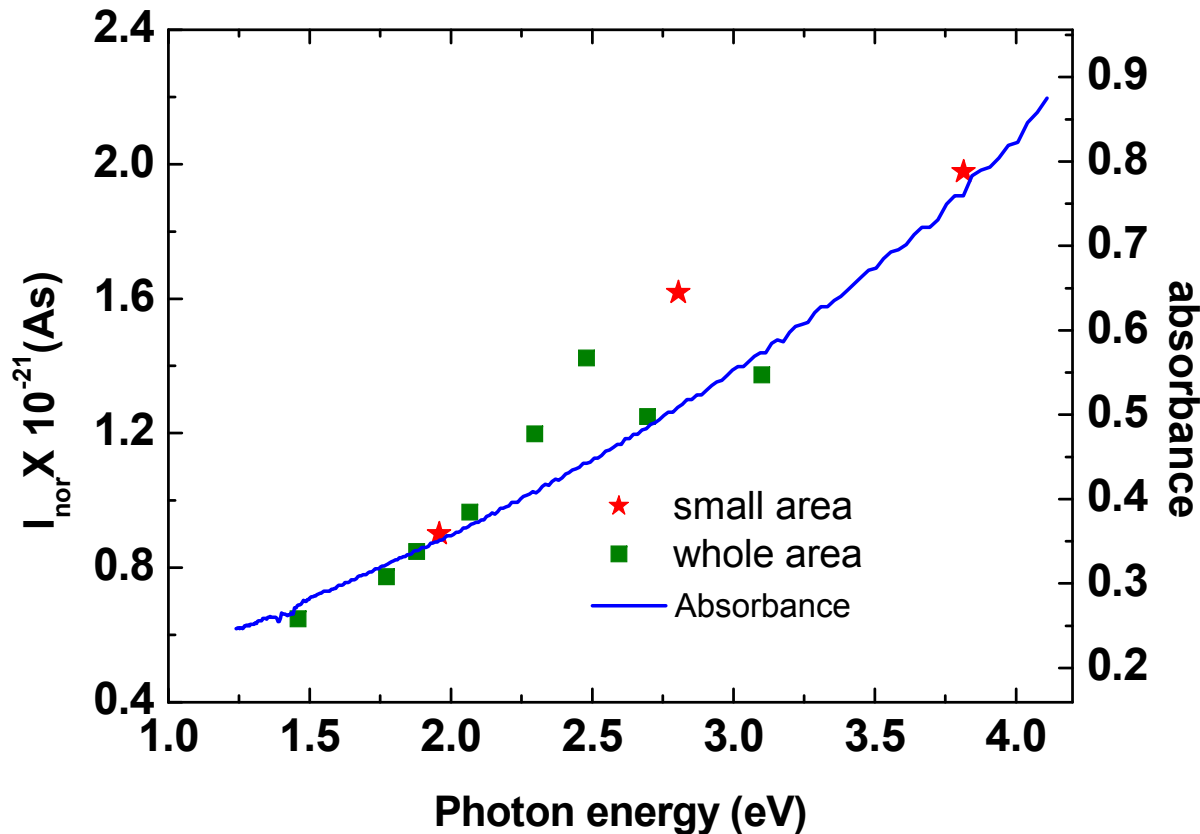
CNT absorbance
(log₁₀ 1/T)

Signals detected with the first carbon nanotube radiation detector



A. Ambrosio et al: "A prototype of a Carbon Nanotube microstrip radiation detector", *Nuclear Instruments and Methods in Physics Research A* 589 (2008) 398–403

Fotocurrent vs λ



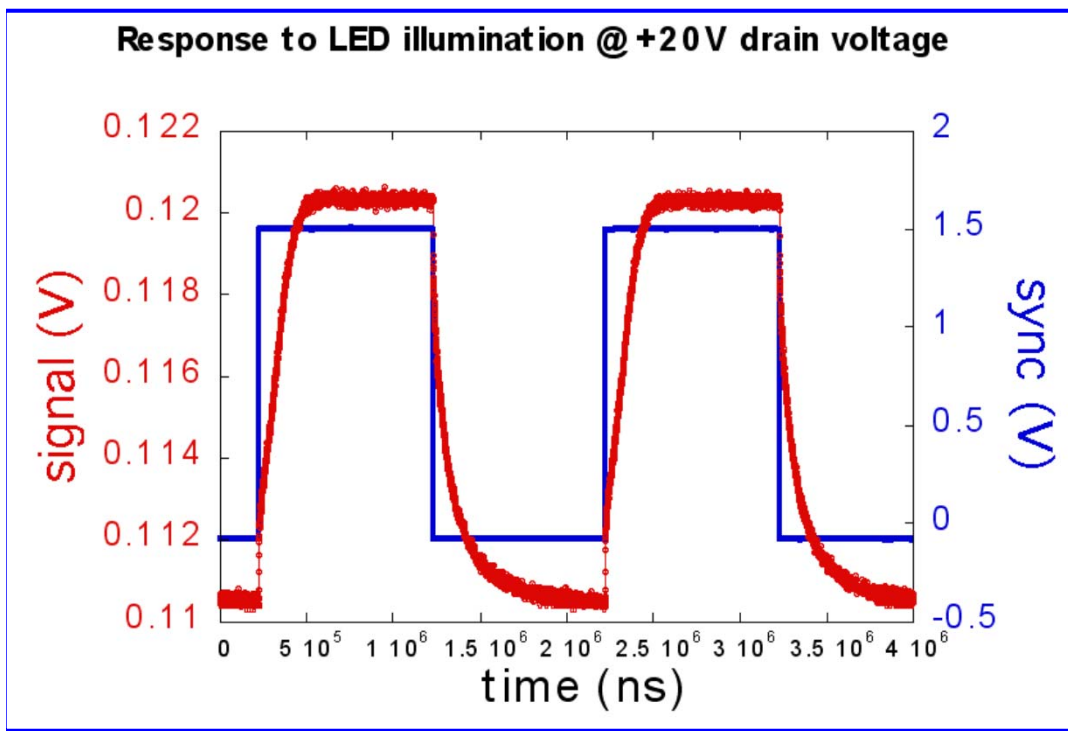
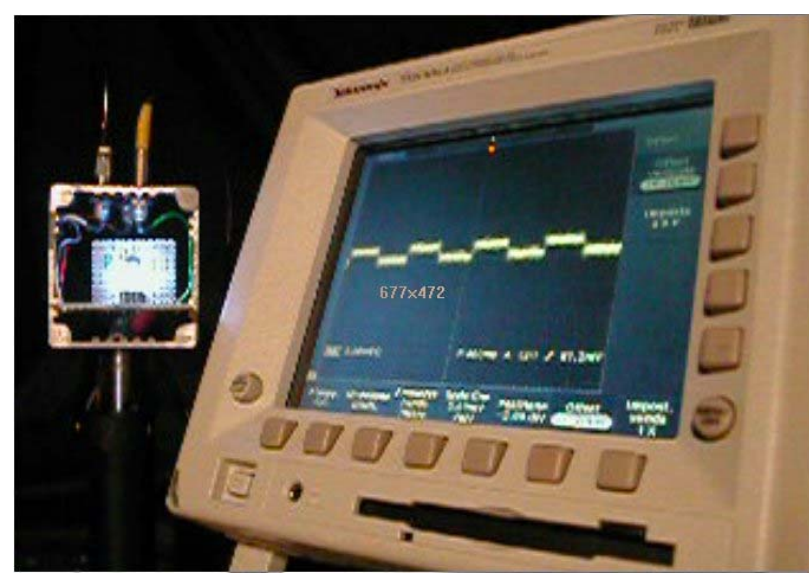
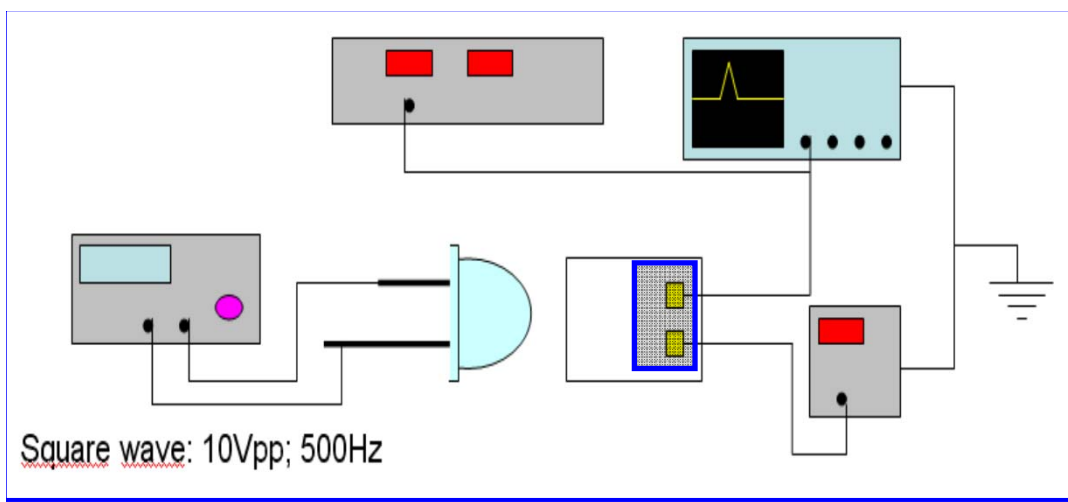
Photocurrent normalized to the number of photons I_{nor} vs photon energy, obtained illuminating the whole surface of a MWCNT sample with filtered light (■) as well as small part of the surface with laser spots (★). Continuous line indicates the absorbance spectrum of the same MWCNT sample

M. Passacantando et al: "Photoconductivity in defective carbon nanotube sheets under ultraviolet-visible-near infrared radiation", *APPLIED PHYSICS LETTERS* 93, 051911 2008



GINT

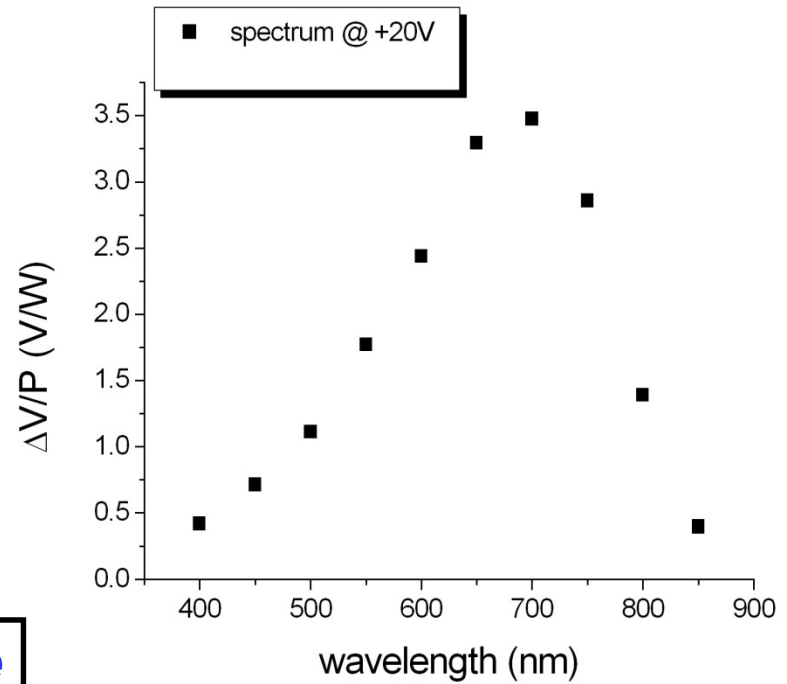
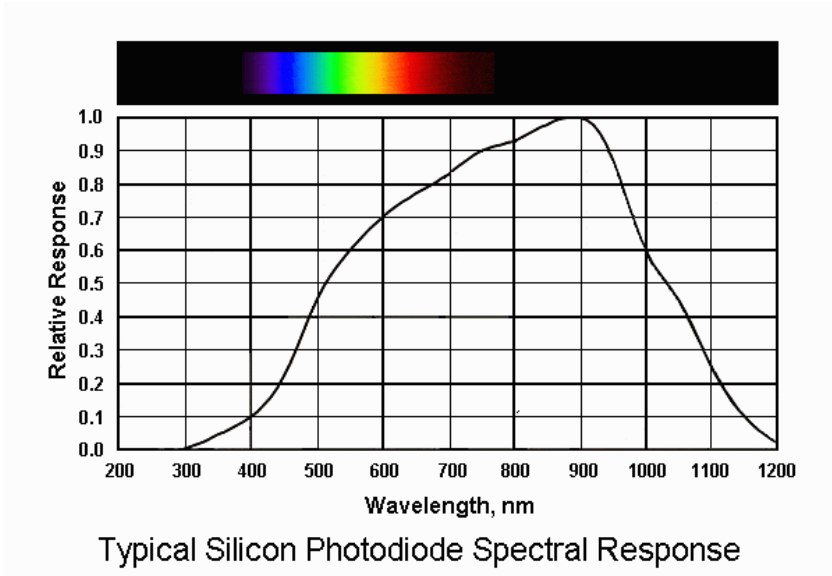
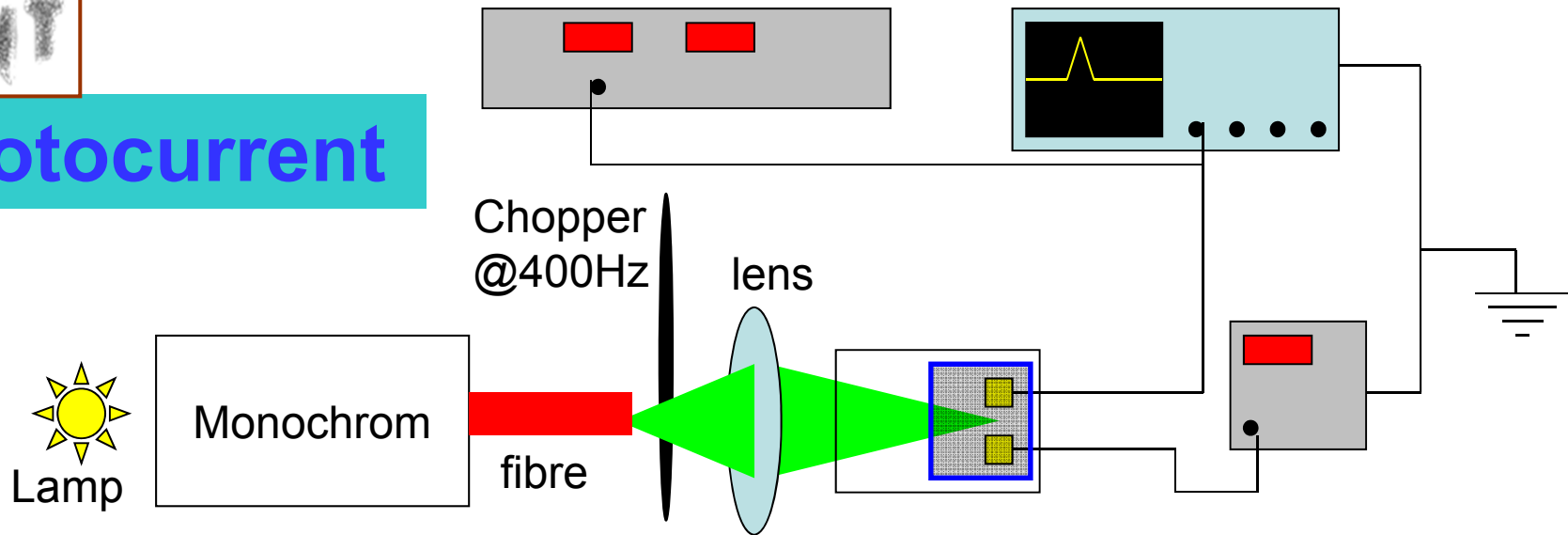
(Gruppo INFN per le NanoTecnologie)



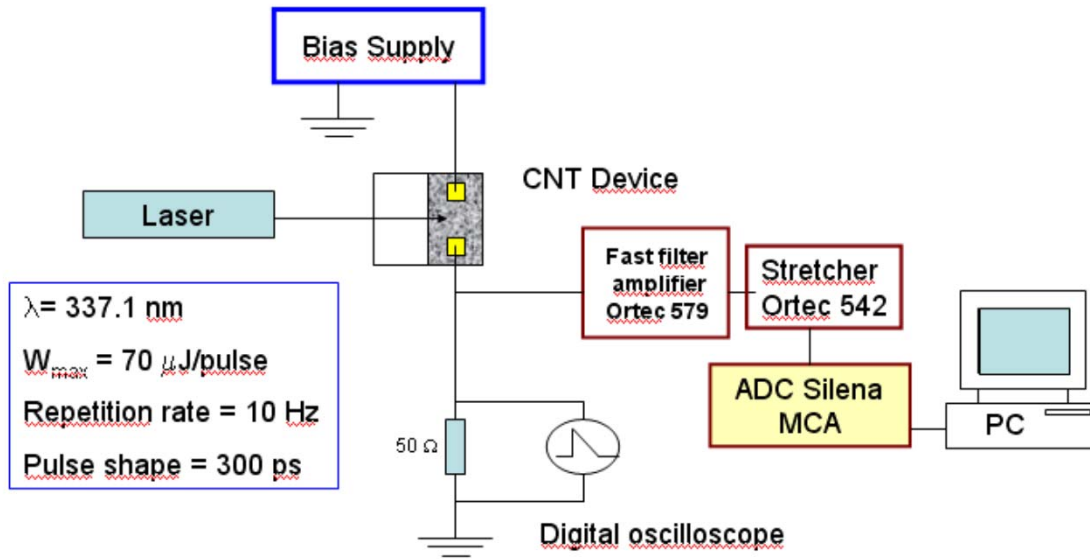
Photocurrent



Photocurrent



CNTs 550°C @ +20V drain voltage



Photocurrent with UV radiation

